

# A Compressed Sampling and Dictionary Learning Framework for WDM-Based Distributed Fiber Sensing

Christian Weiss<sup>1</sup> and Abdelhak M. Zoubir<sup>1</sup>

<sup>1</sup>*Signal Processing Group, Institute of Communications and Graduate School of Computational Engineering,  
Technische Universität Darmstadt, Darmstadt, Germany*

December 9, 2024

## Abstract

We propose a versatile framework that unifies compressed sampling and dictionary learning for fiber-optic sensing. It employs a redundant dictionary that is generated from a parametric signal model and establishes a relation to the physical quantity of interest. Imperfect prior knowledge is considered in terms of uncertain local and global parameters. To estimate a sparse representation and the dictionary parameters, we present a modified alternating-minimization algorithm that is equipped with a pre-processing routine to handle strong dictionary coherence. The performance is evaluated by simulations and experimental data for a practical system with common core architecture.

## 1 Introduction

Fiber-optic sensors have paved the way to a wide range of sensing applications based on different sensing technologies [62, 85, 52, 51, 61, 63, 24, 37]. Fiber Bragg grating (FBG) sensors are often employed in smart structures for high-resolution quasi-distributed temperature or strain monitoring [23, 75, 45, 68]. In systems based on wavelength-division multiplexing (WDM), fiber interrogation is performed using wavelength-tunable lasers that feature high local signal-to-noise ratios (SNRs). For quasi-distributed sensing, a wide laser tuning range is necessary, besides high sweep rates, to monitor time-varying perturbations such as vibrations [69, 93]. Impairments due to strain and temperature cause a shift in the Bragg wavelengths of the FBGs [52]. At the receiver side, this shift is translated into a shift in the delay of the reflections. In order to infer the quantity or nature of impairments at the FBGs, precise estimation of the reflection delays is important [23, 69, 93].

Constant monitoring at high sweep rates results in large amounts of data to be stored/processed and requires costly high-speed analog-to-digital converters (ADCs). Compressed Sampling (CS) is an emerging technology that addresses these problems [12, 21, 32]. The CS-based acquisition process follows a periodic non-uniform sampling paradigm [57, 64]. In principle, digital and analog CS can be distinguished. The challenge in digital CS is to efficiently *encode* the original signal samples into CS samples without explicitly considering the acquisition process itself [80]. In analog CS, one is interested in realizing compression in the analog domain prior to sampling. There exist serial and parallel hardware architectures using one single or multiple ADCs, respectively [32]. Serial implementations usually require high filter orders and produce correlated output samples that exhibit redundancy due to the convolution process [99]. Therefore, architectures using parallel branches with low-rate ADCs are often preferred [82, 99, 66, 32, 90]. In order to recover the original signal or to extract the desired information from the CS samples, an adequate, efficient and automated signal processing scheme is desirable. CS

---

Submitted on July 30, 2016, to [© 2016 Optical Society of America.] One print or electronic copy may be made for personal use only. Systematic reproduction and distribution, duplication of any material in this paper for a fee or for commercial purposes, or modifications of the content of this paper are prohibited.

recovery algorithms rely on the sparsity of the acquired signal with respect to a certain dictionary. A sparse approximation of the signal is typically estimated by solving an ill-conditioned inverse problem with sparsity constraints and can yield high-resolution estimates [60, 32, 35]. Due to these properties, CS has become a favorable tool in a variety of sensing applications [60, 98, 44, 59, 72, 32, 35, 40, 38]. However, a sparsity-promoting dictionary is the key component in any sparse signal processing method. Popular dictionaries used in the CS literature are based on a classical Fourier or wavelet analysis [21]. Nevertheless, redundant dictionaries gain increasing importance as they are more likely to yield a sparse representation [78]. In fact, they are frequently applied in the context of CS [27, 84, 74]. Composite dictionaries are one type of redundant dictionaries that are composed of different sub-dictionaries and can describe more general signals [31, 27, 42, 19]. A crucial requirement for the success of CS is that the columns of the combined sampling and dictionary matrix exhibit low coherence, especially when sub-optimal sparse approximation methods are employed [29, 78]. The term *coherence* is used to describe the level of similarity between dictionary columns. For redundant dictionaries, matrix pre-conditioning can help to alleviate this problem [19].

Identifying an appropriate dictionary is a non-trivial task. In dictionary learning (DL) the acquired data is used to create a dictionary. Alternating minimization (AM) is a prominent heuristic for iteratively estimating a dictionary along with a sparse representation [5, 2]. In the literature, AM is also known as *block-nonlinear Gauss-Seidel method* or *block coordinate descent method* [13]. Generally, non-parametric and parametric DL (PDL) can be distinguished. Except for some norm-constraints, non-parametric DL methods are unable to exploit available information of the dictionary [6]. In parametric DL, the dictionary is created from a parametric model. Similar to non-parametric methods, the acquired data is used to adapt the dictionary but only its parameters need to be adjusted. If an accurate generative signal model is available, they are superior in matching the structure of certain signals [6]. Moreover, parametric dictionaries allow for an effective representation of large-scale dictionaries and arbitrarily-sized signals. This is the case because only the parameters need to be stored rather than the samples in all dictionary columns [6, 76]. One important example are translation-invariant dictionaries [48, 49, 15] which are created from short generating functions.

In this work, we propose a versatile unified CS and DL (CS-DL) framework for an automated estimation of the reflection delays and dictionary parameters in WDM-based fiber-optic sensing. It combines the advantages of CS with high-resolution quasi-distributed sensing and includes *a priori* available but imperfect knowledge of the signal. We jointly consider several issues of sparse estimation and DL in the CS-DL framework with respect to the target application. These include CS, parametric modeling of the signal using physically motivated or auxiliary parameters, dictionary construction as well as sparse estimation under the unfavorable conditions of strong dictionary coherence and uncertainty. In particular, we employ a sparsity-promoting composite dictionary that constitutes translation-invariant sub-dictionaries and we propose the *coherence distance* as a measure of dictionary coherence for general dictionaries of this structure. We refer to the columns of a dictionary as *atoms*. They are created from a generative parametric model for the reflected signal that relies on a modular linear time-invariant (LTI) system architecture and assumes uncertainty in the model parameters. The locations of the sparse coefficients are directly related to the reflection delays to be estimated. From the acquired samples, the uncertain dictionary parameters are estimated in an iterative DL process that exerts the widely used AM approach. In each AM iteration, sparse reconstruction is performed by a modified orthogonal matching pursuit (OMP) algorithm, where the process of reconstruction and DL is supported by an additional inter-atom interference (IAI) mitigation procedure that maintains the physical correspondence between the locations of the dictionary atoms and the reflection delays. In the CS-DL framework, PDL-OIAI refers to the core algorithm that combines AM-based PDL and OMP-based sparse estimation with IAI mitigation. The efficacy of PDL-OIAI is evaluated in a quantitative performance analysis. Compared to a reference method without IAI mitigation, we obtain accurate sparse representations for moderate SNRs at the cost of a higher computational complexity. For the dictionary parameters, we obtain locally optimal estimates. Finally, the suitability of CS-DL is experimentally validated for a particular system setup, showing that the number of samples and the average sampling rate can be substantially reduced.

## 1.1 Contributions

- (I) We provide a versatile CS-DL framework for WDM-based quasi-distributed fiber-optic sensing that pairs the advantages of CS and PDL. Following a non-uniform sampling paradigm for CS, it abates the average sampling rate and reduces the number of samples to be stored and processed. The relevant information is extracted using only the CS samples and some incomplete prior knowledge of the signal.
- (II) We estimate the reflection delays directly in the sparse domain by identifying a generic parametric dictionary with local and global parameters. As a figure of merit, we introduce the coherence distance to evaluate the level of difficulty of the sparse estimation problem for different parameter settings and high sparsity levels. It can be used for general shift-invariant dictionaries of this structure. We also establish a relation to the more popular Babel function [84].
- (III) At the core of the CS-DL framework, we introduce the PDL-OIAI algorithm as a variant of AM-based sparse estimation and DL. It is used to estimate the reflection delays along with the uncertain dictionary parameters. To handle strong dictionary coherence, PDL-OIAI is equipped with an IAI mitigation routine for dictionary pre-conditioning. This facilitates sparse estimation such that it suffices to use a simple greedy algorithm rather than an optimization-based algorithm. The latter can, in principle, handle stronger dictionary coherence but comes at the cost of a higher computational load. We also analyze the computational complexity in the context of a reference method, PDL-OMP.
- (IV) We show how to tailor the general CS-DL framework to match a specific system setup for WDM-based fiber sensing. To this end, we compile a parametric model for the observed signal that is used to create an explicit application-specific dictionary. This model suits the system setup that was used to produce the experimental data shown for validation.
- (V) We present simulations to assess the performance of PDL-OIAI as compared to PDL-OMP and to the Cramér-Rao lower bound (CRLB) for various scenarios of different dictionary parameter values, CS sampling matrices and SNRs. Finally, these results are supported and verified by using experimental data from a real fiber sensor system.

## 1.2 Related work

To date, only a few sources report the application of CS to WDM-based distributed fiber sensing. This work refines and extends some prior investigations in [87, 88]. Different hardware implementations of analog CS have been proposed. Yu *et al.* [99] point out the problem of high filter orders and sample correlation in serial architectures and investigate a technique to reduce the number of branches in parallel architectures. The work in [66] compares the compatibility of a serial and parallel architecture to Xampling [66, 65, 32], a unified framework for analog CS in which the sampling process is characterized by unions of subspaces. Our considerations rely on a parallel CS architecture. The authors in [57, 64] describe the CS-based acquisition process in terms of a periodic non-uniform sampling paradigm. Termed *multi-coset* sampling, this has been theoretically investigated for blindly estimating the spectral support of multiband signals [64]. In our proposed CS-DL framework, non-uniform sampling is described by a sparse sampling matrix that is created from the *Database-Friendly* (DF) distribution [1] to reduce the average sampling rate and, possibly, the number of parallel ADC branches.

There exist several approaches to learning a sparsity-promoting dictionary from the acquired data. Popular AM-based DL algorithms for non-parametric dictionaries are provided in [33, 3, 81]. In [33], the family of iterative least-squares DL algorithms is presented. Aharon *et al.* propose another iterative method, called K-SVD [3]. DL based on the recursive least-squares algorithm is introduced in [81] and also robust approaches exist [22, 58, 41]. In these works the dictionary itself, however, is non-parametric. Besides AM, a conceptionally different method is presented, e.g. in [43], where a Bayesian framework is adopted to jointly estimate the sparsity level and the sparse coefficients along

with unknown dictionary parameters. In our work, however, we pursue the AM paradigm. Design methods for parametric dictionaries are proposed in [92, 6], where the dictionary is subjected to minimum-coherence constraints. In contrast to these works, our dictionary is not explicitly restricted by such constraints. Instead, it is based on a parametric model that accounts for the underlying physical processes and the quantities to be estimated (reflection delays). To compensate for the dictionary coherence, we incorporate an additional IAI mitigation step in the PDL-OIAI algorithm. The problem of dictionary coherence in sparse estimation is investigated in [29, 78], where optimal sensing dictionaries are derived with respect to popular coherence measures such as the *mutual coherence* and the *Babel function* (also called *cumulative coherence*). However, it is found that the performance gain in these methods is limited because no information of the acquired data is used [29, 94]. In PDL-OIAI, we exploit such information by applying an adaptive method for IAI mitigation, proposed in [94]. It adopts a minimum-interference distortionless response (MIDR) approach to derive the new dictionary atoms. To create an explicit parametric dictionary matrix, the authors in [56, 95] use a parametric model for the received signal. Extending these ideas, we consider a parametric dictionary that is composed of different sub-dictionaries and assume uncertainty in its parameters. Dictionaries with a composite structure have been theoretically investigated in terms of uniqueness of the sparse representation for pairs of orthonormal bases [31]. This theory is further elaborated for multiple and more general types of dictionaries in [42, 27], where the *spark* of a matrix is used to measure the linear dependence between the dictionary atoms. The work in [19] also investigates redundant sparse representations in the context of CS. We build up on the idea of composite dictionaries by concatenating sub-dictionaries to allow for potentially non-uniform FBGs along the sensing fiber. In fact, the resulting dictionary structure represents one type of translation-invariant dictionaries introduced in [48, 49, 15]. Relying on a modular structure, we instantiate a particular dictionary that suits the experimental setup in [69, 93].

For PDL and sparse estimation, we consider an AM approach which was firstly introduced in [55]. To the benefit of this concept, popular related methods such as K-SVD [3] appeared. For overcomplete dictionaries, algorithms with provable recovery guarantees and convergence bounds have been developed [2, 5]. These methods, however, use AM for learning non-parametric dictionaries. In PDL-OIAI, we estimate the parameters of a model that generates the atoms of the dictionary. Other related sparse estimation and PDL approaches are proposed in [9, 7, 36, 54, 73]. The method in [9] aims at high-resolution parameter estimation with joint model order estimation based on common information criteria. A static dictionary is created from closely spaced (only global) parameter samples and the estimates are obtained by solving an  $\ell_p$ -regularized least-squares ( $\ell_p$ -RLS) sparse estimation problem with  $p < 1$  to account for high dictionary coherence. Based on this approach, the method in [7] can additionally adjust the dictionary parameters according to the measured data and, therefore, overcome the problem of parameter quantization in static dictionary-based estimation. The effect of parameter quantization is also considered in [36], where the authors apply polar interpolation between adjacent dictionary atoms in order to avoid an increased atom coherence that would result from a refined dictionary grid. The method in [7] is similar to PDL-OIAI in that an AM scheme is used to successively estimate, first, the sparse coefficients using an  $\ell_p$ -RLS algorithm and, subsequently, the dictionary parameters by solving a least-squares optimization problem with constraints on the parameter spacing to restrict the dictionary coherence. Both approaches in [9, 7] also estimate the model order and involve the solution of a non-convex optimization problem, which is not guaranteed to obtain a globally optimal solution. Our proposed method, in turn, has perfect knowledge of the model order (number of FBGs). To handle severe dictionary coherence, we do not explicitly restrict the atom coherence but include an IAI mitigation step for dictionary pre-conditioning. Thus, a computationally more efficient greedy method with a fixed number of iterations can be used for sparse estimation. The PDL approach in [54] considers uncertain dictionary parameters in terms of unknown wall-locations in a multipath environment for through-the-wall-radar imaging. A mixed  $\ell_1$ - $\ell_2$  norm optimization problem is formulated to estimate the unknown parameters along with the sparse target reflectivities. It requires solving a nested optimization problem with inner convex and outer non-convex sub-problems, which becomes computationally complex when the number of parameters increases. This technique is extended in [73], where a network of radar systems is used to estimate an indoor scattering scene. Scene

reconstruction and wall parameter estimation is performed in a distributed fashion across the network, using an AM-based approach for multipath exploitation. However, no dictionary pre-conditioning such as IAI mitigation is applied and only global parameters are considered.

### 1.3 Outline

The remainder of this article is organized as follows: Section 2 introduces the working principle and basic setup of WDM-based quasi-distributed fiber sensing. Section 3 describes how CS is performed in this setting and introduces the generic parametric dictionary structure. Requirements, algorithms, and the CRLB for sparse estimation are briefly reviewed before the problem of dictionary coherence is described qualitatively and also quantitatively in terms of the coherence distance. In Section 4, the CS-DL framework and the PDL-OIAI/OMP algorithms are presented. Further, IAI mitigation is explained and the computational complexity of the overall algorithm is analyzed in comparison with the reference method, PDL-OMP. Next, in Section 5, the CS-DL framework is truncated to suit a particular system setup by compiling a parametric signal model and specifying a dictionary that follows the proposed generic structure. The performance of PDL-OIAI/OMP is evaluated in simulations and experimentally validated using real data. A discussion of the results and findings is provided in Section 6. Section 7 concludes this work.

## 2 System Setup and Sensing Principle

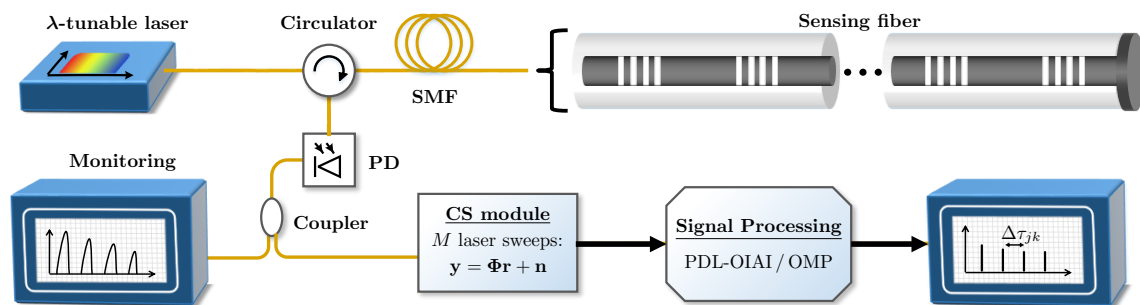


Figure 1: Basic system layout for WDM-based quasi-distributed fiber-optic sensing with CS-based acquisition, followed by sparse estimation and DL using the PDL-OIAI or PDL-OMP algorithm.

At first, we describe the essential components of the considered core architecture based on the fiber sensing system in [69, 93]. We assume a modular architecture in which additional components may be added in terms of an LTI model. Subsequently, we briefly review the sensing principle and specify the quantities to be retrieved from the CS samples.

### 2.1 Basic setup

Let us consider the system in Fig. 1 which is based on the experimental setup in [69, 93]. The core system is extended by a CS acquisition module and a signal processing block. The employed wavelength-tunable laser is assumed to operate in pulsed mode. The emitted signal travels through a single-mode fiber (SMF) into the sensing fiber. If the emitted wavelength falls into the reflection bandwidth of an FBG, it is reflected back to the receiver. A circulator redirects the signal towards the photodetector (PD), where it is converted to the electrical domain. For the purpose of visualization, a coupler may send one portion of the signal, e.g. 10%, to a monitoring unit and the rest to the CS acquisition module. Finally, the desired information is extracted from the acquired CS samples using PDL-OIAI/OMP (see Section 4).

## 2.2 Impairment monitoring using FBGs

FBGs reflect light within a narrow region around their Bragg wavelength,  $\lambda_B = 2n_{\text{eff}}\Lambda_{\text{FBG}}$  [67], where  $n_{\text{eff}}$  is the effective refractive index of the propagating mode and  $\Lambda_{\text{FBG}}$  is the grating period (grating pitch). They are transparent to other wavelengths. The reflection spectra of the FBGs along the sensing fiber are assumed to have a well-separated spectral support and may exhibit a non-uniform shape. Moreover, any impairments at one FBG are assumed to be uniformly distributed along its spatial extent. For vibration monitoring, this is fulfilled if the acoustic wavelength of a vibration signal is much larger than grating length [25]. Then, the grating period is uniformly stretched/compressed, resulting in a shift of  $\lambda_B$  by  $\delta\lambda_B$  which indicates the effective quantity of impairments. This shift can be caused by strain,  $\epsilon_s$ , or temperature change,  $\Delta T$ . It is given by

$$\frac{\delta\lambda_B}{\lambda_B} = P_e\epsilon_s + [P_e(\alpha_s - \alpha_f) + \eta_t]\Delta T, \quad (1)$$

where  $P_e$  is the strain-optic coefficient,  $\alpha_s$ ,  $\alpha_f$  are the thermal expansion coefficients of the fiber bonding material and the fiber itself, respectively, and  $\eta_t$  is the thermo-optic coefficient [70, 50, 97]. Changes in strain and temperature are *a priori* indistinguishable, unless the strain component varies considerably faster than the temperature. However, if the temperature and strain coupling coefficients of two adjacent gratings are known, it is possible to recover both quantities without ambiguity [97].

## 2.3 Quantifying impairments from time delays

When the lasing wavelength is swept through the entire wavelength region,  $R_{\text{sw}}$ , of the gain medium, pulses at varying center wavelength are launched into the sensing fiber. The single pulses are reflected if their spectral support overlaps with the reflection region of FBG $_k$ ,  $k = 1, \dots, K$ . In order to avoid ambiguities, we require that the spatial distance of the FBGs to the receiver increases with  $k$ , and that  $\lambda_{B,k} \ll \lambda_{B,k+1} \forall k$ . Then, each reflection can be uniquely assigned to a single FBG. Due to a limited bandwidth of the PD and the receiver circuitry, the individual laser pulses are usually not resolved and only the envelope modulating the pulses is observed. Let us define FBG $_j$ ,  $j \in \{1, \dots, K\}$ , as a reference point which is located in a controlled environment and never subject to perturbations. For a constant sweep rate,  $S_r$ , the reflected envelopes arrive with delays  $\tau_k$ ,  $k = 1, \dots, K$ , where  $\tau_j$  is the delay associated with the reference point. Then,

$$\Delta\tau_{jk} = |(\tau_k \pm \delta\tau_k) - \tau_j|, \quad (2)$$

is the differential delay and  $\delta\tau_k$  is the absolute delay-shift induced by impairments acting at FBG $_k$ . By precisely estimating  $\delta\tau_k$  (or  $\Delta\tau_{jk}$ ), we can infer  $\delta\lambda_k \forall k \in \{1, \dots, K\} \setminus j$  by [69]

$$\delta\lambda_{B,k} = \delta\tau_k S_r R_{\text{sw}}. \quad (3)$$

The amount of strain or temperature change is then obtained from (1). When time-varying perturbations are monitored,  $S_r$  has to be much faster than the perturbation frequency. However, we assume that the observed scene is stationary during the CS acquisition process.

## 3 Compressed Sampling for Fiber Sensing

The fundamental assumption in CS is that, for a signal  $\mathbf{r} \in \mathbb{C}^N$ , there exists a dictionary matrix  $\mathbf{A} \in \mathbb{C}^{L \times N}$ ,  $N \geq L$ , with entries  $\{\mathbf{a}_n\}_{n=1}^N$  called *atoms*, in which  $\mathbf{r}$  is sparsely represented [12]:

$$\mathbf{r} = \sum_{n=1}^N x_n \mathbf{a}_n = \mathbf{A} \mathbf{x}. \quad (4)$$

$\mathbf{x} \in \mathbb{C}^N$  is a sparse coefficient vector in which all but  $K$  entries are zero. Then,  $\mathbf{r}$  is said to be  $K$ -sparse in  $\mathbf{A}$  [12]. Note that we assume CS to be performed in the analog domain. For simplicity,

however, we use a discretized model that lives within a finite-dimensional Euclidean space to describe the received signal and the dictionary. Nevertheless, this notation can be extended to linear operators and projections of generalized vectors in the Hilbert space  $\mathcal{L}_2$  of square-integrable functions. In (4),  $\mathbf{r}$  may represent the Nyquist samples of the received sensor signal  $r(t) \in \mathcal{L}_2$ . It is often encountered in practice that  $\mathbf{x}$  is not exactly sparse but contains no more than  $K$  significant non-zero components [35]. Then,  $\mathbf{r}$  is said to be *compressible* with respect to  $\mathbf{A}$ , and can be approximated by sparse reconstruction techniques.  $\mathbf{A}$  may be a unitary transformation or a redundant representation of a subspace (*redundant* dictionary) [30]. CS-based acquisition can be described by a sampling matrix  $\Phi$ , with rows  $\{\phi_m^T\}_{m=1}^M$  that define  $M \ll N$  projections, i.e. [12]

$$\mathbf{y} = \sum_{m=1}^M \phi_m^T \mathbf{r} + \mathbf{n} = \Phi \mathbf{A} \mathbf{x} + \mathbf{n} := \mathbf{B} \mathbf{x} + \mathbf{n}. \quad (5)$$

$\mathbf{B} := \Phi \mathbf{A} \in \mathbb{C}^{M \times N}$  is the combined sensing matrix and  $\mathbf{y} \in \mathbb{C}^M$  contains the compressed samples (CS samples). Herein,  $\mathbf{n}$  is the noise component which is assumed to be zero-mean white Gaussian with variance  $\sigma_n^2$ . Since the data is real-valued, we only deal with real-valued vectors and matrices. During each laser sweep, we can acquire the samples described by a single row in  $\Phi$ . Therefore,  $M$  sweeps are required to complete the total acquisition process. Moreover, the observed scene is assumed to be stationary during the acquisition time which is determined by  $M/S_r$ . Since  $M \ll L$ , the number of samples to be stored and processed is significantly reduced. By using  $M$  parallel ADCs to realize uniform sampling at rate  $1/T_s$ , where  $T_s$  is the sampling period, each ADC can work at the lower rate  $1/(MT_s)$  [82]. Non-uniform sampling further reduces the average sampling rate and is achieved when  $\Phi$  is a sparse matrix.

### 3.1 Generic parametric dictionary for delay estimation

We consider a composite shift-invariant dictionary structure to estimate the time-delays of the reflections. First, let us define the total observation time of one sweep by  $T_{\text{sw}}$  and divide the observation interval,  $I_{\text{sw}}^{(m)} = [t_m, t_m + T_{\text{sw}}]$ ,  $m = 1, \dots, M$ , of the  $m$ -th sweep into  $K$  non-overlapping segments, where  $t_m + T_{\text{sw}} < t_{m+1}$ . The  $k$ -th segment is represented by a set of delays,  $\mathcal{T}_k$ ,  $k = 1, \dots, K$ , which defines the maximally considered delay range of a reflection from FBG $_k$ . Hence, a reflection with delay  $\tau_k$  in (2) can be uniquely assigned to FBG $_k$ . Let  $\Omega = \{1, \dots, N\}$  be the total set of dictionary indices and let  $\mathbf{A}_k$  denote the sub-dictionary for the  $k$ -th segment of  $I_{\text{sw}}^{(m)}$ . The index subset associated with  $\mathbf{A}_k$  is

$$\Omega_k = \{n \in \Omega \mid N_{k-1} \leq n \leq N_k\}, \quad k = 1, \dots, K, \quad (6)$$

where  $N_{k+1} > N_k$  with  $N_0 = 1$ ,  $N_K = N = |\Omega|$ . To keep notations simple, we accredit the same number of grid points to each segment and choose  $N$  such that  $|\Omega_k| = (N/K) \in \mathbb{N}_+ \forall k$ . Now let  $r_k(t)$  be the (continuous) reflection from FBG $_k$ , centered around  $t = 0$ . The entries of each atom in  $\mathbf{A}_k$  can be formed by a sampled and delayed version of  $r_k(t)$ , i.e.

$$[\mathbf{a}_n]_l = r_k(lT_d - n\delta t), \quad n \in \Omega_k, \quad l = 1, \dots, L, \quad (7)$$

where  $T_d$  is the design sampling period. The delay spacing,  $\delta t > 0$ , determines the grid granularity, where  $N\delta t \leq LT_s \leq T_{\text{sw}}$  has to hold. For  $n \in \Omega_k$ ,  $\mathbf{a}_n$  is associated with a delay  $\tau_k \in \mathcal{T}_k$ , where the set of delays

$$\mathcal{T}_k = \{\tau \in \mathbb{R}_+ \mid \tau = (n-1)\delta t, n \in \Omega_k\} \quad (8)$$

corresponds to the  $k$ -th segment of an observation interval  $I_{\text{sw}}^{(m)}$ . The complete composite shift-invariant dictionary structure becomes

$$\mathbf{A} = [\mathbf{A}_1, \dots, \mathbf{A}_k, \dots, \mathbf{A}_K]. \quad (9)$$

Hence, the absolute time delays ( $\tau_k \pm \delta\tau_k$ ) of the observed reflections correspond to the locations (support) of the non-zero components in  $\mathbf{x}$ , i.e.  $\text{supp}\{\mathbf{x}\} = \{n \in \Omega \mid x_n \neq 0\}$ . Alternatively, the relative delays  $\Delta\tau_{jk}$  in (2) can be estimated, e.g. by using FBG $_1$  as a reference point and by defining the delay

of its reflection,  $\tau_1$ , as the zero-delay point.

A parametric dictionary can be constructed when  $r(t)$  is described by a parametric model. Due to imperfect prior knowledge of the signal and the dictionary, we introduce uncertain global parameters,  $\boldsymbol{\theta}_G$ , and/or local parameters,  $\boldsymbol{\theta}_{L_k}$ ,  $k = 1, \dots, K$ . An example of a global parameter can be the effective receiver bandwidth. Local parameters can be related to the shape of the reflection spectrum of individual FBGs. Then, an atom associated with  $\mathbf{A}_k$  is denoted by  $\mathbf{a}_n(\boldsymbol{\theta}_k)$ ,  $n \in \Omega_k$ , where  $\boldsymbol{\theta}_k = [\boldsymbol{\theta}_G, \boldsymbol{\theta}_{L_k}]^T$ . Defining  $\boldsymbol{\theta} = [\boldsymbol{\theta}_G, \boldsymbol{\theta}_{L_1}, \dots, \boldsymbol{\theta}_{L_K}]^T$ , the complete parametric dictionary structure is given by

$$\mathbf{A}(\boldsymbol{\theta}) = [\mathbf{A}_1(\boldsymbol{\theta}_1), \dots, \mathbf{A}_k(\boldsymbol{\theta}_k), \dots, \mathbf{A}_K(\boldsymbol{\theta}_K)] . \quad (10)$$

For notational convenience, we may drop the parameters in the argument but include them whenever it is necessary.

### 3.2 Sparse estimation: Methods, guarantees and the CRLB

In order to obtain a solution for  $\mathbf{x}$ , we have to solve the equation system in (5). However, since  $M \ll N$ , the problem is ill-posed and there exist infinitely many solutions. A unique solution can be obtained by imposing appropriate constraints. As  $\mathbf{x}$  is sparse by assumption, sparse solutions are clearly favorable. They can be obtained by greedy or optimization-based methods. Optimization-based methods cast (5) as a (usually convex) optimization problem with sparsity constraints.  $\ell_1$ -minimization [35] is widely used to obtain globally optimal solutions with robustness to measurement errors and noise, but the computational complexity can be high. We employ a greedy OMP-based approach, where sparsity is imposed by iteratively choosing one atom that exhibits maximum correlation with the residual signal. The reasons for this choice are threefold: Firstly, as a greedy method, it is simple and fast, given that  $K \ll N$  [17, 35]. Secondly, the number of iterations equals the sparsity level  $K$ , of the signal [100, 35]. For the dictionary in (10),  $K$  also corresponds to the number of reflections, i.e. the number of FBGs, which is exactly known. Thirdly, since the reflection delays are continuous, it is likely that they fall in between two grid points defined by the dictionary. Optimization-based method tempt to compensate this by selecting two adjacent atoms with reduced amplitudes, which misleadingly indicates two reflections. OMP only selects one atom in each iteration and is guaranteed to yield a  $K$ -sparse approximation after  $K$  iterations.

The success of sparse reconstruction depends on certain joint conditions on  $\mathbf{B}$ ,  $K$  and  $\mathbf{x}$ . A popular quality measure is the *restricted isometry property (RIP)* [20, 18, 35]

$$(1 - \delta)\|\mathbf{x}\|_2^2 \leq \|\mathbf{B}\mathbf{x}\|_2^2 \leq (1 + \delta)\|\mathbf{x}\|_2^2 , \quad (11)$$

where  $\delta \geq 0$  is called restricted isometry constant. Given  $\mathbf{B}$ ,  $\delta$  can be computed for a certain sparsity level  $K$ . For many sparse reconstruction algorithms, including  $\ell_1$ -minimization and OMP, there exist upper bounds,  $\delta^*$ , that guarantee successful sparse reconstruction. To estimate a  $K$ -sparse signal using OMP,  $\mathbf{B}$  is required to fulfill the RIP of order  $K + 1$  with isometry constant  $\delta < 1/(3K^{1/2}) = \delta^*$  [26]. Thus, standard OMP fails if the dictionary coherence is too strong [78, 94]. While it is still an open problem to explicitly construct (in polynomial time) a deterministic matrix that meets the necessary conditions for CS, it can be shown that sub-Gaussian random matrices fulfill the RIP at a given sparsity level with high probability [12, 35].

#### 3.2.1 The constrained CRLB

In order to assess the sparse estimation performance, it is desirable to have a benchmark in terms of achievable theoretical bounds. A popular measure is the *constrained* Cramér-Rao lower bound (CRLB). It describes a lower bound for the variance of any unbiased estimator,  $\hat{\mathbf{x}}_{\text{ub}}$ , in a sparse setting and is given by [14]

$$\text{CRLB: } E\{\|\hat{\mathbf{x}}_{\text{ub}} - \mathbf{x}\|_2^2\} \leq \sigma_n^2 \text{Tr}([\mathbf{B}_{\mathcal{S}}^T \mathbf{B}_{\mathcal{S}}]^{-1}), \|\mathbf{x}\|_0 = K. \quad (12)$$

Herein,  $\mathbf{B}_{\mathcal{S}}$  is a submatrix of  $\mathbf{B}$  that consists of only the columns with indices in  $\mathcal{S} := \text{supp}\{\mathbf{x}\}$  and  $\text{Tr}(\cdot)$  denotes the trace operator on a matrix. The lowest value of the CRLB, i.e.  $K \sigma_n^2$ , is achieved

when the columns in  $\mathbf{B}$  are orthogonal (see Appendix A). It can be shown [14] that the constrained CRLB is equal to the CRLB of the *oracle estimator* which has perfect knowledge of  $\mathcal{S}$ .

### 3.3 Redundant dictionaries and coherence measures

Redundant dictionaries have two major advantages: firstly, the existence of a sparse representation becomes more likely as the number of dictionary atoms increases [78]. Secondly, redundancy allows for high-resolution estimation of quantities directly in the sparse domain [60, 94]. We employ the redundant dictionary in (10) to obtain high-precision estimates of reflection delays. Despite their advantages, overcomplete dictionaries face the problem of atom coherence. That is,  $\mathbf{B} = \mathbf{\Phi}\mathbf{A}$  may no longer meet the necessary requirements to guarantee stable and robust sparse reconstruction [27, 35, 19]. Since  $\mathbf{\Phi}$  is a random matrix, let us assume that it fulfills the RIP with respect to  $\mathbf{A}$  and neglect the aspect of CS for now. Hence, we regard the problem of estimating a sufficiently sparse representation of the signal from the redundant dictionary  $\mathbf{A}$ , such that  $\mathbf{\Phi}$  fulfills the RIP with respect to  $\mathbf{x}$ . In particular, we require that the support  $\mathcal{S} = \text{supp}\{\mathbf{x}\}$  is correctly identified since it represents the reflection delays to be estimated. In fact, verifying the RIP is NP-hard, so other measures have been proposed that are easier to calculate in practice. They often consider the coherence between dictionary atoms.

#### 3.3.1 The mutual coherence

The mutual coherence is a widely used measure to quantify the similarity between dictionary atoms [28, 84, 35]. It is given by

$$\mu(\mathbf{A}) = \max_{j \neq i} |\mathbf{a}_j^H \mathbf{a}_i| = \max_{j \neq i} |[\mathbf{A}^H \mathbf{A}]_{ji}|, \quad j, i \in \Omega. \quad (13)$$

and reflects the most significant correlation between all pairs.

#### 3.3.2 The Babel function

A more generalized incoherence measure, known as the Babel function or  $\ell_1$ -coherence, is introduced in [27, 84] and defined by

$$\mu_B(\mathbf{A}, s) = \max_{|\Lambda|=s} \max_{i \in \Omega \setminus \Lambda} \sum_{j \in \Lambda} |\mathbf{a}_i^H \mathbf{a}_j| \leq s \mu(\mathbf{A}). \quad (14)$$

It takes into account the dictionary subset  $\Lambda \subset \Omega$ , with cardinality  $|\Lambda| = s$ , that exhibits the maximum cumulative correlation with all other dictionary atoms  $\mathbf{a}_i$ ,  $i \in \Omega \setminus \Lambda$ . The function  $\mu_B(\mathbf{A}, s)$  is non-decreasing in  $s$ , where  $\mu_B(\mathbf{A}, 1) = \mu(\mathbf{A})$ . A dictionary is called *quasi-incoherent* if the Babel function increases “slowly” in  $s$  [84]. Using the *exact* recovery condition [84], OMP recovers an ideally  $K$ -sparse signal if

$$\mu_B(\mathbf{A}, K-1) + \mu_B(\mathbf{A}, K) < 1. \quad (15)$$

For more general signals, however, a good  $K$ -sparse *approximation* is desired. The authors in [39, 84] show that, if the dictionary is sufficiently incoherent, OMP is an efficient approximation algorithm for finding a good  $K$ -sparse representation which is close to the best  $K$ -sparse representation of a signal.

#### 3.3.3 The coherence distance

Considering the dictionary in (10), a strong overlap of adjacent dictionary atoms may result from a small  $\delta t$  or from an unlucky parametrization,  $\boldsymbol{\theta}$ . In this case, and especially when  $K$  is small,  $\mu_B(\mathbf{A}(\boldsymbol{\theta}), s)$  and  $\mu(\mathbf{A}(\boldsymbol{\theta}))$  do not change much for small variations in  $\delta t$  or  $\boldsymbol{\theta}$ . Yet, this can have strong impact on the level of difficulty in finding the correct sparse support. Therefore, to evaluate the level of difficulty of a sparse estimation problem for different parameter settings, it is desirable to have an alternative coherence measure that emphasizes this issue. The coherence distance is an appropriate

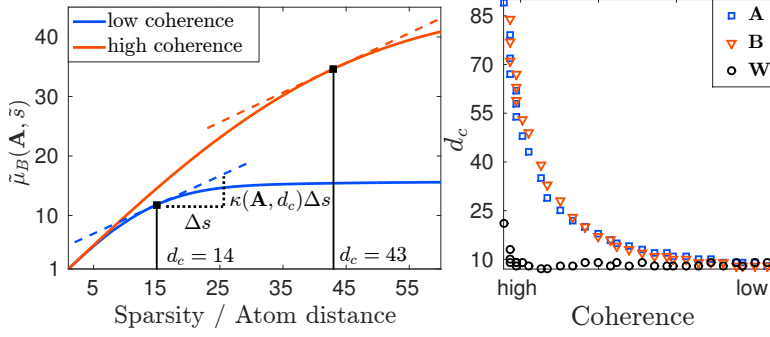


Figure 2:  $\mu_B(\mathbf{A}, s)$  and  $d_c(\mathbf{A})$  for high and low coherence levels (left) and  $d_c$  as a function of the coherence level for different matrices:  $\mathbf{A}$ ,  $\mathbf{B}$  and  $\mathbf{W}$  (right).

measure for general dictionaries of the form (10), where the similarity between atoms decreases with increasing index difference. Given such dictionary,  $\mathbf{A}$ , and some  $\beta_d > 0$ , we define the coherence distance by

$$d_c(\mathbf{A}, \beta_d) = \max_{i \in \Omega} \left\{ \arg \min_{d=|i-j|} |\mathbf{a}_i^T \mathbf{a}_j| \leq \beta_d |\mathbf{a}_i^T \mathbf{a}_i|, j \in \Omega \right\}, \quad (16)$$

where  $|\mathbf{a}_i^T \mathbf{a}_i| = 1 \forall i \in \Omega$  by convention.  $d_c(\mathbf{A}, \beta_d)$  corresponds to the smallest difference of atom indices for which the coherence decreases by a factor  $\beta_d$  with respect to the atom self-coherence. Let us calculate  $\mu_B(\mathbf{A}, s+1)$  and establish a relation to  $d_c(\mathbf{A})$ . For a structured dictionary as in (10), we choose  $\Lambda$  in (14) to be a set of  $s+1$  adjacent indices, i.e.  $\Lambda = \{q \in \Omega \mid q_0 \leq q \leq q_0 + s\}$ . Then, choosing any  $i^* \in \Omega \setminus \Lambda$  directly adjacent to  $\Lambda$ , i.e.  $|i^* - q_0| = 1$  or  $|q_0 + s - i^*| = 1$ , maximizes the expression in (14) for any  $q_0 \in \{2, \dots, N - s - 1\}$ . We define a continuous extension of  $\mu_B(\mathbf{A}, s)$  by  $\tilde{\mu}_B(\mathbf{A}, \tilde{s})$ ,  $\tilde{s} \in \mathbb{R}_+$ , and choose  $i^* = q_0 - 1$ . Then, we obtain a 1st-order approximation

$$\mu_B(\mathbf{A}, s+1) = \sum_{j=1}^{s+1} |\mathbf{a}_{i^*}^T \mathbf{a}_{i^*+j}| \approx \mu_B(\mathbf{A}, s) + \kappa(\mathbf{A}, s) \Delta s, \quad (17)$$

where

$$\kappa(\mathbf{A}, s) = \frac{d\tilde{\mu}_B}{d\tilde{s}}(\mathbf{A}, \tilde{s})|_{\tilde{s}=s}. \quad (18)$$

Setting  $\Delta s = 1$ , we find that  $\kappa(\mathbf{A}, s) \Delta s \geq |\mathbf{a}_{i^*}^T \mathbf{a}_{i^*+s+1}|$  since  $\mu_B(\mathbf{A}, s)$  is concave, and obtain the immediate correspondence

$$d_c(\mathbf{A}, \beta_d) = \arg \min_{d \in \Omega} \{ \kappa(\mathbf{A}, d) \leq \beta_d |\mathbf{a}_{i^*}^T \mathbf{a}_{i^*+d}|, i^* + d \leq N \}. \quad (19)$$

Thus, with the above assumptions on the dictionary structure,  $d_c(\mathbf{A}, \beta_d)$  is equivalent to the sparsity level  $s$ , where  $\tilde{\mu}_B(\mathbf{A}, \tilde{s})$  grows at a rate  $\kappa(\mathbf{A}, d_c) \leq |\mathbf{a}_{i^*}^T \mathbf{a}_{i^*+d}| / \beta_d < \kappa(\mathbf{A}, d_c - 1)$ . Subsequently, we always use  $\beta_d = 0.5$  and drop the arguments of  $d_c(\mathbf{A}, \beta_d)$  when the context is clear. For  $\beta_d = 0.5$ ,  $d_c$  signifies the index difference at which the atom coherence is decreased by 3 dB with respect to the atom self-coherence. Fig. 2 (left) depicts the evolution of  $\tilde{\mu}_B(\mathbf{A}, \tilde{s})$  in  $\tilde{s}$  and its relation to  $d_c(\mathbf{A}, \beta_c = 0.5)$  when  $\mathbf{A}$  exhibits strong and low coherence, respectively. As stated before, the slope of  $\tilde{\mu}_B(\mathbf{A}, \tilde{s})$  is very similar for both coherence levels when  $\tilde{s} < 10$ , whereas  $d_c$  takes very different values. Thus, when  $K$  is small,  $d_c$  emphasizes the difference in the coherence level of a dictionary for varying parametrizations,  $\boldsymbol{\theta}$ . It can be used to quantify the level of difficulty of estimating  $\mathcal{S} = \text{supp}\{\mathbf{x}\}$ . Fig. 2 (right) shows the values of  $d_c$  at various coherence levels and for different matrices:  $\mathbf{B}$  inherits much from the structure of the original dictionary  $\mathbf{A}$ . Therefore, their coherence distance takes similar values.  $\mathbf{W}$  is a modified dictionary that results from the IAI mitigation procedure described in Section 4. It turns out that  $d_c(\mathbf{W})$  takes significantly lower values which eases the sparse estimation process.

## 4 The CS-DL Framework

In this section we introduce the CS-DL framework for WDM-based quasi-distributed fiber sensing. It combines CS-based acquisition with sparse estimation and DL using strongly coherent parametric dictionaries with uncertainty. Fig. 3 depicts a structure diagram of CS-DL. For CS, a sub-Gaussian matrix can be employed, where sparse binary matrices allow for a simple hardware realization and reduce the average sampling rate. At the core of CS-DL, we introduce an AM-based algorithm, *PDL-OIAI*, that uses the CS samples to iteratively estimate the reflection delays  $\mathcal{S} = \text{supp}\{\mathbf{x}\}$ , together with the uncertain dictionary parameters  $\boldsymbol{\theta}$ . An additional IAI mitigation step is performed to handle strong dictionary coherence. We refer to *PDL-OMP* as a reference method in which IAI mitigation is omitted. The computational complexity is analyzed at the end of this section.

### 4.1 The PDL-OIAI algorithm: AM-based sparse estimation and DL for highly coherent parametric dictionaries

We aim at solving problem (5) for  $\mathbf{x}$  in cases where the dictionary is highly coherent and where some of the dictionary parameters contain uncertainty due to incomplete prior knowledge. PDL-OIAI is a modified AM algorithm that uses the CS samples to estimate  $\mathbf{x}$ , and in particular  $\text{supp}\{\mathbf{x}\}$ , along with  $\boldsymbol{\theta}$  when the dictionary is highly coherent. In each iteration, the estimated dictionary parameters of the previous iteration are used to further improve the sparse estimates (reflection delays). While direct sparse estimation methods aim at estimating the total dictionary,  $\mathbf{B}(\boldsymbol{\theta}) = \Phi \mathbf{A}(\boldsymbol{\theta})$ , PDL-OIAI uses the CS samples,  $\mathbf{y}$ , associated with  $\mathbf{B}$ , to estimate parameters of the concatenated dictionary,  $\mathbf{A}(\boldsymbol{\theta})$ . Unlike the conceptually similar algorithms in [73, 7], PDL-OIAI incorporates IAI mitigation in the AM-based estimation procedure to yield a modified sensing dictionary with reduced atom coherence. This permits us to use a simple OMP-based algorithm with low complexity for the actual sparse estimation task. Further, the number of FBGs determines the model order and, hence, the sparsity level, which also equals the number of required OMP iterations. For both, convex optimization-based and greedy approaches, dictionary pre-conditioning might be necessary to fulfill the requirements for correct sparse estimation. Once a dictionary with sufficient incoherence is available, different sparse estimation algorithms may be used. The performance of various methods has been comprehensively studied in the CS literature. Thus, such comparison is not in the focus of this work. Instead, we aim at highlighting the benefits of IAI mitigation in AM-based sparse estimation and PDL, when the dictionary is of the form (10) and no restrictions are imposed on the atom coherence during construction. Using a simple greedy sparse estimation method in PDL-OIAI minimizes the computational complexity that is added on top of dictionary pre-conditioning. Later on, we show that the sparse estimation performance of PDL-OIAI is close to the CRLB. It is therefore comparable to the performance of the  $\ell_p$ -RLS method in [7], which involves the solution of a non-convex optimization problem. In order to underline the performance gain due to IAI mitigation in AM-based PDL, we define a reference method, called PDL-OMP, that directly applies OMP-based sparse estimation without IAI mitigation. Fig. 3 shows a flow diagram of the processing chain for both algorithms. They are initialized using a set of CS samples,  $\mathbf{y}$ , a maximum number of DL iterations,  $D$ , and the combined matrix,  $\mathbf{B} = \Phi \mathbf{A}$ , with an initial guess of the dictionary parameters,  $\hat{\boldsymbol{\theta}}^{(0)}$ . PDL-OIAI adopts the IAI mitigation method in [94] to reduce the coherence distance of  $\mathbf{B}$ . It yields a modified *sensing dictionary*,  $\mathbf{W}$ , that maintains the physical interpretation of the sparse support with respect to  $\mathbf{A}$ . That is, the original sensor signal can be estimated by  $\mathbf{A}\hat{\mathbf{x}}$ , where  $\hat{\mathbf{x}}$  is estimated using  $\mathbf{W}$ , and  $\hat{\mathcal{S}} := \text{supp}\{\hat{\mathbf{x}}\}$  contains the appropriate delay estimates. Subsequently,  $\boldsymbol{\theta}$  is estimated by minimizing the residual,  $\text{res} := \text{res}(\boldsymbol{\theta})$ . In Fig. 3 we use the  $\ell_2$ -norm to calculate the residual, but any other suitable objective function may be used. The pre-defined range of possible parameter values is initially defined according to prior knowledge and physical limitations. This scheme yields locally optimal parameter estimates as it cannot be guaranteed that the parameter ranges form a convex set, and also the objective function of the residual may not be jointly convex in all uncertain parameters. In the  $d$ -th iteration, the estimates  $\hat{\boldsymbol{\theta}}^{(d)}$  are used to obtain an improved estimate  $\hat{\mathbf{x}}^{(d+1)}$  which, in turn, yields an improved estimate  $\hat{\boldsymbol{\theta}}^{(d+1)}$ . The algorithms terminate when  $\text{res}^{(d)}$  is below a threshold or after  $d = D$  iterations. The threshold can

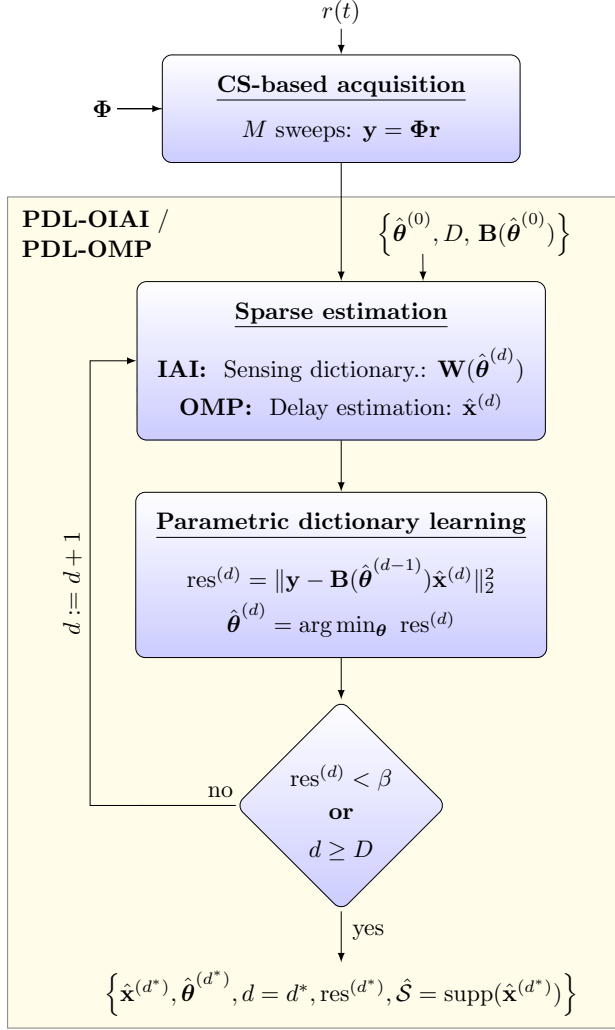


Figure 3: Structure diagram of the CS-DL framework: CS-based acquisition followed by PDL-OIAI/OMP for AM-based sparse estimation and PDL. PDL-OMP does not perform IAI.

be set to  $\beta = (1 + \epsilon_r)P_n$  with  $\epsilon_r > 0$ , where  $P_n$  is an estimate of the total noise power. Ultimately, the iteration index  $d = d^*$ , associated with the smallest residual, is determined to output the final solutions  $\hat{\mathbf{x}}^{(d^*)}$ ,  $\hat{\boldsymbol{\theta}}^{(d^*)}$  and  $\hat{\mathcal{S}} := \text{supp}\{\hat{\mathbf{x}}^{(d^*)}\}$ .

#### 4.1.1 IAI mitigation

We briefly review the concept of IAI mitigation in [94]. It is adopted in PDL-OIAI to ease the task of sparse estimation from highly coherent dictionaries. In contrast to the methods in [29, 78], it also takes the received data into account. The coherence of the combined matrix  $\mathbf{B}$  originates from the coherence of  $\mathbf{A}$  (Fig. 2 (right)). Therefore, IAI mitigation is applied to  $\mathbf{B}$  directly to yield a modified sensing dictionary. OMP suffers from IAI which lies in its conceptual approach to sparse estimation. OMP attempts to iteratively identify the atoms in  $\mathbf{B} = [\mathbf{b}_1, \dots, \mathbf{b}_N]$  that minimize the residual signal. In the *first* iteration ( $k = 1$ ), an atom is selected by solving [94]

$$\max_{i \in \Omega} |\mathbf{b}_i^T \mathbf{y}| = \max_{i \in \Omega} \left| \sum_{q \in \mathcal{S}} \mathbf{b}_i^T \mathbf{b}_q x_q + \mathbf{b}_i^T \mathbf{n} \right|, \quad (20)$$

where we are interested in determining the non-zero components  $x_q \neq 0$ . The sum-term in (20) describes interference with other atoms  $\mathbf{b}_q$ ,  $q \in \mathcal{S}$ , which leads to the selection of incorrect atoms. Thus, instead of (20), Yang *et al.* [94] suggest to solve

$$\max_{i \in \Omega} \left| \sum_{q \in \mathcal{S}} \mathbf{w}_i^T \mathbf{b}_q x_q + \mathbf{w}_i^T \mathbf{n} \right|, \quad (21)$$

where  $\mathbf{w}_i$ ,  $i = 1, \dots, N$ , are the atoms of the modified sensing dictionary,  $\mathbf{W}$ . For  $i \in \mathcal{S}$ , the purpose of  $\mathbf{w}_i$  is to minimize IAI with other *correct* atoms  $\mathbf{b}_j$ ,  $j \in \mathcal{S} \setminus \{i\}$ , while maintaining the correlation with  $\mathbf{b}_i$ . This can be achieved using the minimum interference distortionless response (MIDR) approach in [94], i.e. by choosing  $\mathbf{w}_i$  such that

$$\min_{\mathbf{w}_i} \left| \mathbf{w}_i^T \mathbf{B}_S \mathbf{B}_S^T \mathbf{w}_i \right| \quad s.t. \quad \mathbf{b}_i^T \mathbf{w}_i = 1, \quad i = 1, \dots, N. \quad (22)$$

$\mathbf{B}_S$  contains the columns of the true support which is unknown. Therefore,  $\mathbf{B}_S \mathbf{B}_S^T$  is iteratively approximated by  $\mathbf{B} \mathbf{U}^{(j)} \mathbf{B}^T$ , where  $\mathbf{U}^{(j)} = \text{diag}(|(\mathbf{W}^{(j-1)})^T \mathbf{y}|^\rho)$ ,  $j \in \{1, \dots, J\}$  is an iteration index and  $\rho > 0$  is a regularization parameter. There exists a closed-form solution for each  $\mathbf{w}_i^{(j)}$ ,  $i = 1, \dots, N$ , that is gradually improved in  $J$  internal iterations with initialization  $\mathbf{W}^{(0)} = \mathbf{B}$  (see [94] for details). In subsequent OMP iterations ( $k > 1$ ),  $\mathbf{y}$  has to be replaced by the current residual,  $\mathbf{g}^{(k)}$ ,  $k = 1, \dots, K$ , where  $\mathbf{g}^{(0)} := \mathbf{y}$ . The constraint in (22) ensures that the physical relation between the reflection delays and  $\mathcal{S}$  is maintained. That is,  $\mathbf{r}$  can be estimated by  $\hat{\mathbf{r}} = \mathbf{A} \hat{\mathbf{x}}$ , where  $\hat{\mathbf{x}}$  is a solution to  $\mathbf{y} = \mathbf{W} \mathbf{x}$ , and  $\hat{\mathcal{S}} = \text{supp}\{\hat{\mathbf{x}}\}$  contains appropriate delay estimates. As shown in Fig. 2 (right), for the final sensing dictionary  $\mathbf{W} := \mathbf{W}^{(J)}$ , we find  $d_c(\mathbf{W}) \ll d_c(\mathbf{B})$  such that the correct atoms can be identified at the cost of a higher computational complexity.

## 4.2 Computational Complexity

PDL-OIAI/OMP performs  $D$  AM iterations, i.e. sparse estimation and subsequent PDL. For sparse estimation using OMP, both algorithms require  $K$  iterations according to the considered sparsity level of  $\mathbf{x}$  (number of FBGs), where each iteration has complexity  $\mathcal{O}(NM)$ . Thus, in the sparse estimation step of the  $d$ -th AM iteration,  $d = 1, \dots, D$ , PDL-OMP has complexity  $\mathcal{O}(KMN)$ . However, the complexity of PDL-OIAI, in the  $k$ -th OMP iteration, is dominated by calculating  $\mathbf{w}_i$  in (22)  $\forall i = 1, \dots, N$ , which has complexity  $\mathcal{O}(N^2M + NM^2 + M^3)$ . This step is repeated in  $J$  internal iterations (usually  $J < 10$ ) to improve the quality of  $\mathbf{W}$  for IAI mitigation. Then, in the sparse estimation step of the  $d$ -th AM iteration, PDL-OIAI has complexity  $\mathcal{O}(KJ(N^2M + NM^2 + M^3))$ . As stated in [94], a significant speedup can be achieved by calculating  $\mathbf{W}$  only once for  $k = 1$ , although this results in a lower performance. Moreover,  $\mathbf{w}_i$  can be calculated independently  $\forall i = 1, \dots, N$ , which is efficiently implemented using parallel processing.

In the  $d$ -th AM iteration, sparse estimation is followed by PDL. A closed-form solution for  $\theta$  is not generally available. Therefore, the residual can be locally minimized for each  $\theta_p$ ,  $p = 1, \dots, P$ , by varying its value through a set of possible values,  $\mathcal{R}_{\theta_p}$ , with  $|\mathcal{R}_{\theta_p}| = R_{\theta_p}$ , while keeping all other parameters fixed. The parameter grid may be equally spaced or created with a parameter distance based on the Fisher information that ensures a locally constant inter-atom coherence [8]. For simplicity, let us assume an equal number of grid points, i.e.  $R_{\theta_p} = R_\theta \forall p = 1, \dots, P$ . The complexity of computing the residual for one value  $\theta_p \in R_\theta$  is  $\mathcal{O}(NM^2)$ . Hence, in the PDL step of the  $d$ -th AM iteration, PDL-OIAI/OMP both have complexity  $\mathcal{O}((R_\theta NM^2)^P)$ . Table 1 summarizes the overall computational complexity of PDL-OIAI and PDL-OMP.

## 5 Performance Evaluation in Simulations and Experimental Validation Using Real Data

It is time to apply the CS-DL framework to a particular WDM-based distributed sensing system. We compile a parametric model for the received signal to construct a specific instance of the parametric

Table 1: Computational complexity of PDL-OMP and of PDL-OIAI when  $\mathbf{W}$  is determined  $\forall k = 1, \dots, K$ , or fixed for  $k > 1$ .

<b>PDL-OMP:</b> $\mathcal{O}(D[KNM + (R_\theta NM^2)^P])$
<b>PDL-OIAI:</b> $\mathcal{O}(D[KJ(N^3M + N^2M^2 + NM^3) + (R_\theta NM^2)^P])$
<b><math>\rightarrow \mathbf{W}</math> fixed:</b> $\mathcal{O}(D[J(N^3M + N^2M^2 + NM^3) + KNM + (R_\theta NM^2)^P])$

dictionary in (10). Then, we use simulations to evaluate the performance of PDL-OIAI and PDL-OMP for the considered system in various scenarios of different sampling matrices, dictionary parameter values and SNRs. Finally, we provide some experimental validation by applying CS-DL to real sensor data using the same parametric model/dictionary.

## 5.1 A parametric signal model for CS-DL

To apply CS-DL in practice, a modular system architecture is considered. Extending the work in [87], we adopt and compile existing physical models to express the received sensor signal and to construct a specific instance of the parametric dictionary in (10). Modularity means that each component has a well-defined input/output relation. We further assume that the subsystem between laser and photodetector can be described by an (LTI) system. Thus, the model is generic and applicable to a wider class of system configurations since other linear components may be added, removed or interchanged. In particular, we present a model for the basic system architecture in [69, 93], which is schematically depicted in Fig. 1, and examine CS-DL for that system. The individual components are described below.

### 5.1.1 Laser output:

The authors in [69, 93] have developed a special class of  $\lambda$ -tunable lasers. Their advantages for distributed fiber sensing are three-fold: firstly, no tunable filters are required which keeps the hardware complexity low. Secondly, a wide tuning bandwidth is available to serve a large number of FBGs. Thirdly, high sweep rates are achieved, where the wavelength varies linearly with the frequency of the modulation current. The emitted light at the center wavelength  $\lambda$  can be described in the baseband frequency domain by a chirped Gaussian pulse of the form [69, 93, 83]

$$A^{(\lambda)}(\omega) \sim \exp\left(-\frac{\omega^2}{2(\delta\omega)^2}\right), \quad (23)$$

with a wavelength-dependent bandwidth

$$\delta\omega = \sqrt{\pi \frac{f_m}{\lambda}} \left( \frac{8\pi c_0 \Gamma_a}{|D_{\text{DCF}}^{(\lambda)}| L_{\text{DCF}}} \right). \quad (24)$$

$c_0$  is the speed of light and  $L_{\text{DCF}}$  is the length of the dispersion compensating fiber (DCF) which forms the laser cavity.  $\Gamma_a$  denotes the amplitude modulation index of the light within the DCF and  $D_{\text{DCF}}^{(\lambda)}$  is the first order dispersion parameter. The latter can be determined by a 5th-order Sellmeier fit to the measured group delay [16, 71]. A semiconductor optical amplifier (SOA) is used as a gain medium and  $f_m$  is the modulation frequency of the injection current. The  $i$ -th emitted laser pulse is comprised of the superimposed cavity modes around the instantaneous center wavelength,  $\lambda_i$ . At index  $i$ , the instantaneous pulse repetition rate is given by  $\tau_{\text{rep},i} = 1/f_{m,i}$ . The sum of all pulses forms the output signal corresponding to one laser sweep. This signal is modulated by the wavelength-dependent gain profile of the SOA. It can be described by [89, 10]

$$g^{(\lambda)} = \frac{a_1(N_c - N_0) - a_2(\lambda - \lambda_{N_c})^2 + a_3(\lambda - \lambda_{N_c})^3}{1 + \epsilon_c P_{\text{av}}}, \quad (25)$$

where  $\epsilon_c$  is called compression factor,  $P_{av}$  is the average output power over the length of the SOA,  $N_c$  is the actual carrier density and  $N_0$  is the carrier density at the transparency point (no-gain wavelength). In (25),  $\lambda_N$  and  $\lambda_0$  are the maximum gain wavelengths corresponding to  $N_c$  and  $N_0$ , respectively. The difference  $\lambda_{N_c} - \lambda_0$  is due to the carrier difference  $N_c - N_0$ , while  $a_1$  accounts for the carrier difference with respect to the transparency point and  $a_2$  characterizes the spectral width of the gain profile with asymmetry indicated by  $a_3$ . Note that  $a_{1,2,3}$  can be determined by a 3rd-order fit to the measured SOA gain. In subsequent simulations, we have used some of the values listed in [89, 10].

### 5.1.2 Fiber transmission:

The transfer function of a standard single-mode fiber (SMF) of length  $L_{SMF}$  can be derived from a Taylor expansion of the propagation constant  $\beta^{(\lambda)}$ , where we neglect any non-linear effects by assumption. Since the FBGs are located at different positions along the sensing fiber, the travel distance varies in  $\lambda$ , i.e.  $L_{SMF}^{(\lambda)}$ . Denoting the damping by  $\alpha^{(\lambda)}$  and the 2nd- and 3rd-order terms of the Taylor expansion of  $\beta^{(\lambda)}$  by  $\beta_2^{(\lambda)}$  and  $\beta_3^{(\lambda)}$ , respectively, the baseband transfer function becomes [77, 79, 47]

$$H^{(\lambda)}(\omega, L_{SMF}^{(\lambda)}) = \exp\left(-\left(\alpha^{(\lambda)} + j\frac{\beta_2^{(\lambda)}}{2}\omega^2 + j\frac{\beta_3^{(\lambda)}}{6}\omega^3\right)L_{SMF}^{(\lambda)}\right). \quad (26)$$

$\beta_{2,3}^{(\lambda)}$  are related to the dispersion,  $D_{SMF}^{(\lambda)}$ , and to its slope,  $S_{SMF}^{(\lambda)} = (d/d\lambda)D_{SMF}^{(\lambda)}$  [79], while the damping is modeled by [63]

$$\alpha^{(\lambda)} = A_R \frac{1}{\lambda^4} + B + C^{(\lambda)}. \quad (27)$$

$A_R$  denotes the Rayleigh scattering coefficient,  $B$  accounts for other wavelength-independent losses such as microbending or waveguide imperfections and  $C^{(\lambda)}$  describes other wavelength-dependent losses such as  $\text{OH}^-$  absorption peaks. These parameters can be determined by a least-squares fitting to the measured damping. A detailed model for  $C^{(\lambda)}$  is also available in [63].

### 5.1.3 FBG reflection:

We consider uniform (non-chirped) FBGs that are modeled by a periodic perturbation of the refractive index along the fiber core in propagation ( $z$ -) direction [86, 50]:

$$n_c(z) = n_0 + \Delta n_c \left( \frac{2\pi(z - z_0)}{\Lambda_{FBG}} \right), \quad z \in [z_0, z_0 + L_G], \quad (28)$$

where  $L_G$  is the total grating length,  $z_0$  is the grating location,  $n_0$  is the average refractive index within one spatial period  $\Lambda_{FBG}$ , and  $\Delta n_c$  is the perturbation amplitude. Using coupled-mode theory [96, 53, 86, 50], the spectral characteristics of an FBG can be derived by calculating solutions for the field amplitudes,  $S(z)$ ,  $R(z)$ , of a mode and an identical counter-propagating mode, respectively. Coupling is achieved by the dielectric perturbation. For a uniform grating, this corresponds to solving a system of two coupled 1st-order ordinary differential equations with constant coefficients and appropriate boundary conditions [34]

$$\frac{dR}{dz} = i\sigma_c R(z) + i\kappa_c S(z); \quad \frac{dS}{dz} = -i\sigma_c S(z) + i\kappa_c^* R(z), \quad (29)$$

which has a closed-form solution. In (29),  $i$  denotes the imaginary unit and  $(\cdot)^*$  the complex conjugate, while  $\sigma_c$  and  $\kappa_c$  are called the DC-/AC-coupling coefficients. They are proportional to the refractive index. The ratio  $\rho^{(\lambda)} = S(z = z_0)/R(z = z_0)|_\lambda$  describes the field amplitude reflection coefficient at wavelength  $\lambda$ . Defining  $\gamma_c = (\kappa_c^2 - \sigma_c^2)^{1/2}$ , it is given by [34]

$$\rho^{(\lambda)} = \frac{-\kappa_c \sinh(\gamma_c L_G)}{\sigma_c \sinh(\gamma_c L_G) + i\gamma_c \cosh(\gamma_c L_G)}. \quad (30)$$

To model more sophisticated spectral characteristics, e.g. for non-uniform gratings, including chirp or apodization, a closed form solution can be derived by adopting a piece-wise uniform approach, where the FBG is subdivided into  $M_G$  uniform segments. Then, the field amplitudes are calculated for each segment separately. The final result can be written in matrix form by [34]

$$[R_{M_G}, S_{M_G}]^T = \mathbf{F} [R_0, S_0]^T, \quad (31)$$

where  $\mathbf{F} = \mathbf{F}_{M_G} \cdot \mathbf{F}_{M_G-1} \cdots \mathbf{F}_1$  is the total transition matrix and  $\mathbf{F}_i$ ,  $i = 1, \dots, M_G$ , are the transition matrices of each segment.

#### 5.1.4 Received sensor signal:

The reflected signal travels the same way back to the receiver. Thus,  $H^{(\lambda)}(\omega, L_{\text{SMF}}^{(\lambda)})$  is applied twice. The optical center frequency of the total sweep range is  $\Omega_0 = c_0/\lambda_0$  and the instantaneous center frequency of the  $i$ -th pulse is  $\Omega_i = \Omega_0 - \Delta\omega_i$ , where  $\Delta\Omega_i = c_0(\lambda_i - \lambda_0)/(\lambda_i\lambda_0)$ . Using (23, 25, 26, 30) we obtain a frequency domain expression in the baseband for the received pulse train reflected from an FBG at distance  $L_z$ :

$$E_r(\omega) = \sum_i g_i \rho_i e^{-j\omega\tau_{\text{rep},i}} A_i(\omega - \Delta\Omega_i) H_i(\omega - \Delta\Omega_i, L_z)^2. \quad (32)$$

Index  $i$  indicates the dependence of each term on  $\lambda_i$ . The time-domain signal,  $E_r(t) = E_r(t, \lambda(t))$ , is obtained by taking the inverse Fourier transform of  $E_r(\omega)$ , where  $\lambda(t)$  indicates the temporal evolution of the wavelength. In the photodetection process, the responsivity of the PD,  $R_{\text{PD}}^{(\lambda)}$ , depends on the quantum efficiency of the material,  $\eta_{\text{PD}}^{(\lambda)}$  [4]. Different PD types can be distinguished. For simplicity, we assume a uniform distribution of the intensity,  $I(\mathbf{q}, t)$ , at all locations  $\mathbf{q} \in \mathbb{R}^2$  within the sensitive area,  $A_{\text{PD}}$ , of the PD. Then, the incident power becomes  $P(t) = \int_{A_{\text{PD}}} I(\mathbf{q}, t) dA_{\text{PD}} = |E_r(t)|^2/Z_W$ , where  $Z_W$  is the wave impedance of the medium [4]. The PD output current is [4]

$$i(t) = R_{\text{PD}}^{(\lambda)} P(t) = \frac{q_e \lambda(t) \eta_{\text{PD}}^{(\lambda(t))}}{h c_0} \frac{|E_r(t)|^2}{Z_W}, \quad (33)$$

where  $h$  is Planck's constant and  $q_e$  is the elementary charge [4]. A slow photodiode can demodulate the pulse train envelope. To this end, we model the effective bandwidth of the receiver circuitry,  $\Delta f$ , by a lowpass filter with transfer function  $H_{\text{LP}}(\omega)$ :

$$r(t, \Delta f) = \frac{1}{2\pi} \int_{-\infty}^{\infty} e^{j\omega t} [H_{\text{LP}}(\omega) i(\omega)] d\omega, \quad (34)$$

where  $i(\omega)$  is the Fourier transform of  $i(t)$ . In the ensuing sections, we assume uncertainty in  $\Delta f$  as a global parameter,  $\theta_G$ , which jointly affects the temporal width of the reflections contained in  $r(t, \Delta f)$ . Ultimately, a parametric dictionary,  $\mathbf{A}$ , can be created from  $r(t, \Delta f)$  according to (10).

## 5.2 Simulations

In order to assess the performance of sparse estimation and DL, we have truncated the CS-DL framework to suit the particular architecture in Fig. 1. The basic model parameters have been tuned to match the system in [69, 93]. Recall that  $r(t)$  represents the generating function of the dictionary according to (10). The resulting dictionary is now employed in the simulations below.

### 5.2.1 Scenario and basic settings

We consider a sensing fiber with 3 FBGs. Their Bragg wavelengths are such that two of the temporal reflections are closely spaced. All reflections have a uniform shape, a common amplitude,  $A_x$ , and a temporal width determined by the true value of  $\Delta f$ . As a global dictionary parameter, we estimate  $\Delta f$  in terms of a normalized parameter  $\hat{\theta} = \widehat{\Delta f}/\Delta f$ . An initial value is chosen at random with

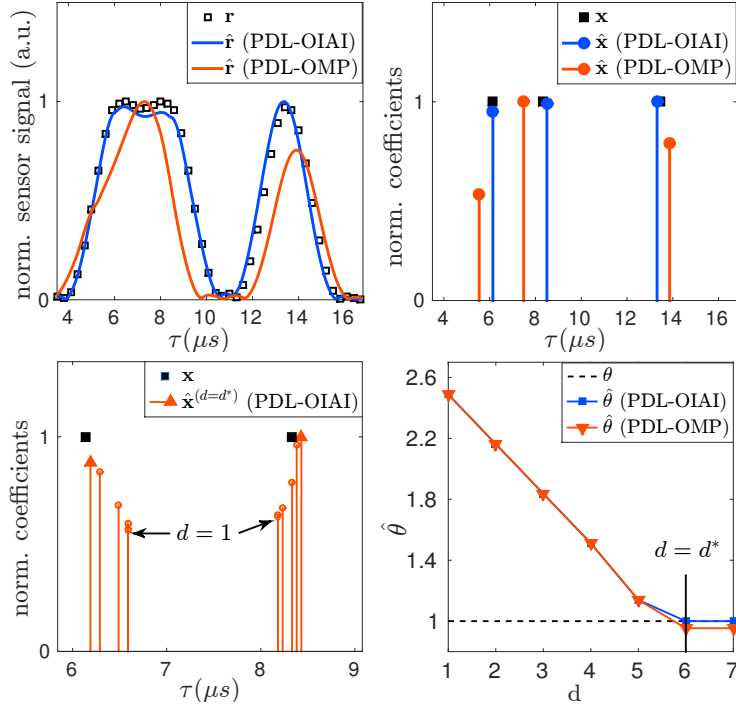


Figure 4: Simulation results for  $d_c = 14$ : Noiseless sensor signal (top left), sparse signal (top right). Black bullets indicate the true delays. Evolution of sparse coefficient estimates (zoomed) vs. iteration index  $d$  (bottom left), and  $\hat{\theta}$  vs.  $d$  (bottom right).

$\hat{\theta}^{(0)} \in [1.2, 5]$  and  $R_\theta < 100$ . The original signal,  $\mathbf{r}$ , has length  $L = 134$  and the dictionary has  $N = 2L$  atoms with a delay resolution of  $\delta t = 50$  ns. CS samples are taken by three types of sampling matrices,  $\Phi$ , with i.i.d. entries drawn from the following random distributions:

- (a) Gauss :  $\mathcal{N}(0, 1)$
- (b) Rademacher :  $\{\pm 1\}$  with equal probability
- (c) DF [1]:  $\{-1, 0, 1\}$  with probabilities  $\{\frac{1}{6}, \frac{2}{3}, \frac{1}{6}\}$ .

PDL-OIAI and PDL-OMP run 3 OMP-iterations to identify  $K = 3$  atoms corresponding to the reflections. PDL-OIAI performs additional  $J = 10$  internal iterations for IAI mitigation. An appropriate regularization parameter,  $\rho$ , is determined in advance. This has to be done once for a particular setting. The sensing dictionary,  $\mathbf{W}$ , is only calculated once in the first OMP iteration to speed up computations (see Section 4.4.2). Also, the form of the CRLB in (12) corresponds to a fixed dictionary. We set the maximum number of AM iterations to  $D = 8$ . The estimation performance is evaluated in terms of the root mean-squared error (RMSE). For some vector  $\mathbf{v}$  and its estimate  $\hat{\mathbf{v}}$ , we define

$$\text{RMSE}(\mathbf{v}, \hat{\mathbf{v}}) = \sqrt{E \{ \|\mathbf{v} - \hat{\mathbf{v}}\|_2^2 \}}, \quad (35)$$

where the expectation operator is replaced by the sample mean over Monte Carlo runs to yield an approximation termed  $\overline{\text{RMSE}}$ .

### 5.2.2 Visualization of PDL-OIAI/OMP: Iterative estimation progress

We use simulated sensor data with an SNR of 10 dB. The coherence distance of the dictionary is  $d_c = 14$ . We take  $M = 94$  CS samples using a Gaussian sampling matrix which reduces the number

of samples to be processed by 30%. Fig. 4 (top left) shows the original samples of the noiseless sensor signal,  $\mathbf{r}$ , and the estimates,  $\hat{\mathbf{r}}$ , obtained by PDL-OIAI/OMP. The sparse signal estimates are depicted in Fig. 4 (top right) and their support indicates the reflection delays. It can be seen that PDL-OMP cannot deal with highly coherent atoms and chooses the wrong support while PDL-OIAI identifies the true support much more accurately. For PDL-OIAI, the sparse support (delay estimates) of the two closely spaced sources are shown in different iteration steps in Fig. 4 (bottom left). We can observe how the estimates for support and amplitudes of  $\mathbf{x}$  improve with increasing iteration index,  $d$ . Fig. 4 (bottom right) shows the evolution of  $\hat{\theta}^{(d)}$  vs.  $d$ . Due to a limited step size per iteration, the slope is linear for  $d < 5$  as both algorithms choose the maximum step-size towards the correct value. PDL-OIAI and PDL-OMP both converge to a final value  $\hat{\theta} \approx \theta = 1$  after  $d^* = 6$  iterations.

### 5.2.3 Performance evaluation

Next, we investigate the empirical performance of PDL-OIAI and PDL-OMP in order to support the previous observations.  $\mathcal{S} = \text{supp}\{\mathbf{x}\}$  is the true sparse support and  $\hat{\mathcal{S}}$  denotes its estimate. The vectors  $\mathbf{s}$  and  $\hat{\mathbf{s}}$  contain, in increasing order, the support and its estimate, respectively. We compare the performance for simulated sensor data generated by two different values of  $\theta$ . The correctly parametrized dictionaries have coherence distances  $d_c = 14$  and  $d_c = 49$ , respectively. Since  $\hat{\theta}^{(0)} > \theta$ , the algorithms start by employing dictionaries with lower coherence distance, i.e.  $\hat{d}_c(\mathbf{A}(\hat{\theta}^{(0)})) < d_c(\mathbf{A}(\theta))$ . Generally, higher values of  $\hat{d}_c$  require more efforts in IAI mitigation. Therefore, the number of internal iterations in PDL-OIAI is set to  $J = 10$  when  $d_c = 14$ , and to  $J = 18$  when  $d_c = 49$ . Usually,  $J < 20$  is sufficient. To determine the average performance, we have carried out 500 Monte Carlo trials for each SNR, for each value of  $\theta \in [1.2, 5]$ , and for each sampling matrix (a)-(c). We first calculate the  $\text{RMSE}(\mathbf{s}, \hat{\mathbf{s}})$  divided by the temporal grid accuracy,  $\delta t$ . It describes the average number of grid points that the estimated support differs from the true support. Then, we compute the  $\text{RMSE}(\theta, \hat{\theta})$  of the estimated dictionary parameter. Finally, we compare the estimation performance for the amplitudes of the non-zero coefficients in  $\mathbf{x}$  with the constrained CRLB in (12) that is calculated for the correctly parametrized  $\mathbf{B}(\theta)$  using sampling matrix (a). Since the constrained CRLB depends on the actual realization of the random matrix  $\Phi$ , its value is averaged over 1000 Monte Carlo trials. Moreover, the constrained CRLB equals the CRLB of the *oracle estimator* which has perfect knowledge of  $\mathcal{S} = \text{supp}\{\mathbf{x}\}$ . Therefore, we only consider the amplitudes in  $\mathbf{x}$  at the true positions in  $\mathcal{S}$ , and the corresponding amplitudes in  $\hat{\mathbf{x}}$  at the estimated positions in  $\hat{\mathcal{S}}$ . Hence, we define  $\mathbf{x}_{\mathcal{S}} := [x_{s_1}, \dots, x_{s_K}]^T = A_x \mathbf{1} \in \mathbb{R}^K$ , where  $s_k \in \mathcal{S}, k = 1, \dots, K$ .  $\mathbf{x}_{\hat{\mathcal{S}}}$  is defined accordingly.

In Fig. 5, we firstly show the  $\text{RMSE}(\mathbf{s}, \hat{\mathbf{s}})/\delta t$ . It can be observed that PDL-OIAI yields more accurate estimates for the reflection delays than PDL-OMP at all SNRs. The difference becomes more significant as  $d_c$  increases but also PDL-OIAI has limited performance when  $d_c$  is too severe. The  $\text{RMSE}(\theta, \hat{\theta})$  indicates that PDL-OIAI and PDL-OMP both perform well in estimating the uncertain dictionary parameter when  $d_c = 14$ . For  $d_c = 49$ , and at low SNRs, the influence of noise dominates the performance of both methods, whereas PDL-OIAI is superior at higher SNRs. Regarding the sparse coefficients, we compare the  $\text{RMSE}(\mathbf{x}_{\mathcal{S}}, \hat{\mathbf{x}}_{\hat{\mathcal{S}}})$ , normalized by the common amplitude  $A_x$ , to the root constrained CRLB (R-CRLB). We find that the estimates of both algorithms cling closely to the R-CRLB when  $d_c = 14$ . However, in the case of  $d_c = 49$ , they both do not yield correct estimates due to restrictive dictionary coherence.

In Fig. 6 and Fig. 7, we show the performance of PDL-OIAI/OMP for the different sampling matrices (a)-(c) when  $d_c = 14$ . The ratio between the number of CS samples and the number of the original samples is  $M/L = 50\%$  in Fig. 6, and only 20% in Fig. 7. This indicates that PDL-OIAI can efficiently extract the desired information from a small number of CS samples when the SNR is high. When  $M/L = 20\%$ , the sparse support is estimated with an average error of  $\text{RMSE}(\mathbf{s}, \hat{\mathbf{s}})/\delta t = 4$  bins at SNR= 20 dB. The average ratio between estimation error and true value of the dictionary parameter goes down to  $\text{RMSE}(\theta, \hat{\theta}) = 6\%$ . Comparing the sparse coefficients to the R-CRLB, a maximum performance loss of  $-20 \lg(\text{RMSE}(\mathbf{x}_{\mathcal{S}}, \hat{\mathbf{x}}_{\hat{\mathcal{S}}})/\text{R-CRLB}) = -9$  dB is observed. Interestingly, although a DF matrix has a high number of zero-projections (2/3 of all samples need not be acquired), similar performance is achieved for all sampling matrices (a)-(c).

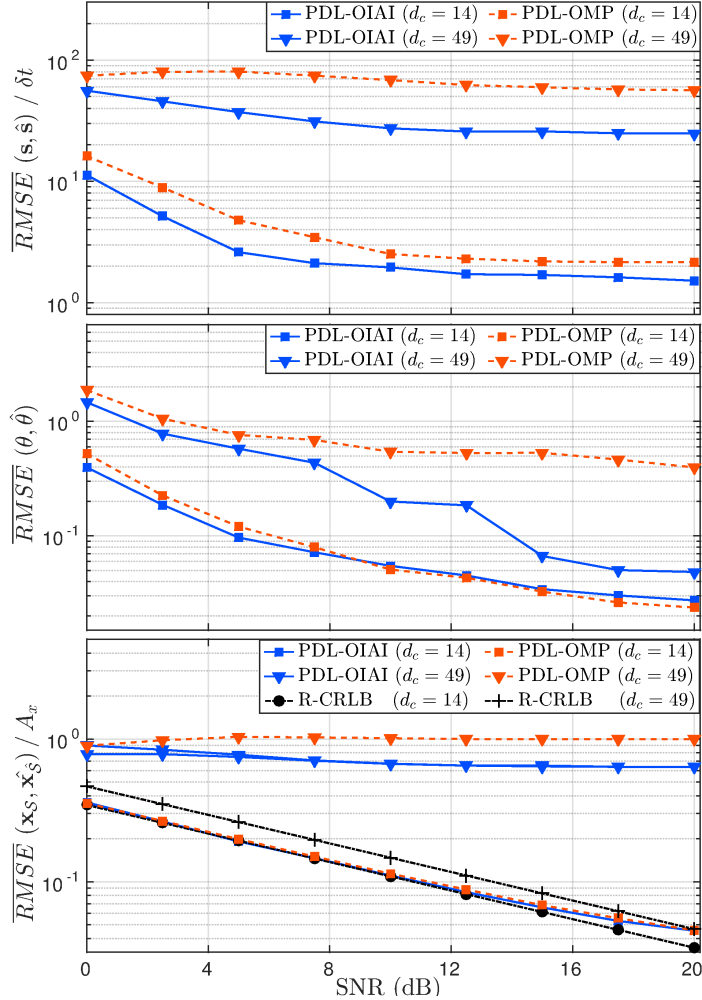


Figure 5: Performance of PDL-OIAI and PDL-OMP for dictionaries with different coherence levels, i.e.  $d_c = 14$  and  $d_c = 49$ .

### 5.3 Experimental validation using real data

Let us now apply the truncated CS-DL framework to experimental data taken from the real reference system in [93, 69] and evaluate the practical performance of PDL-OIAI/OMP for this system. The data was acquired at the Yamashita laboratory of photonic communication devices at The University of Tokyo, Japan. The basic architecture corresponds to the schematic in Fig. 1 and the total experimental setup is detailed in [69, 93]. We tuned the parameters of the model in Section 5.1 to fit the system specifications, the measured spectra of laser output and FBG reflections, and the measured laser output (pulse train) in the temporal domain. We consider  $L = 134$  samples of the received signal,  $\mathbf{r}$ , and take CS samples such that  $M/L = 40\%$ . The dictionary has  $N = 2L$  atoms with a delay spacing of  $\delta t \approx 50$  ns.  $K = 4$  reflections are observed as they are reflected from 4  $\lambda$ -detuned FBGs in the sensing fiber. Their approximate delays are at  $[7.79, 9.05, 10.27, 12.30] \mu\text{s}$  which is potentially off-grid. In PDL-OIAI, we use  $J \leq 8$  iterations for IAI mitigation. To account for the randomness of the sampling matrices, 500 Monte Carlo trials were carried out. Ultimately, confidence intervals were computed for the parameters that fall within the well-defined delay intervals of each FBG. In order to discard outliers that result from an unfortunate conditioning of  $\Phi$ , we show the results in terms of the median and the 85% confidence interval instead of showing mean and standard deviation. The experimentally observed reflections are strongly broadened which, according to the authors in [69], probably arises

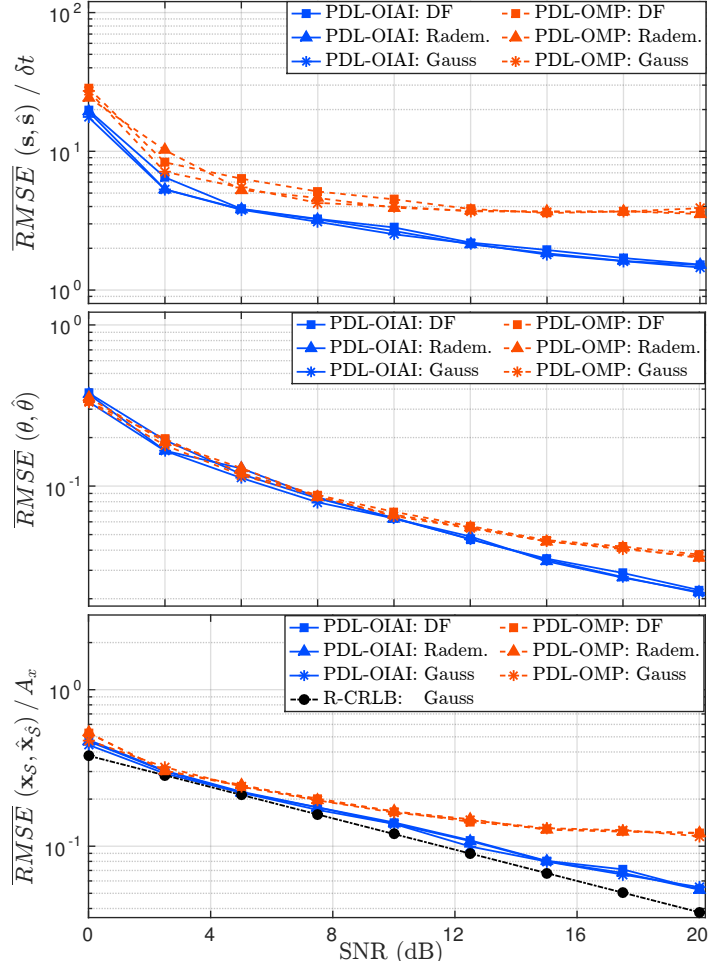


Figure 6: Performance of PDL-OMP and PDL-OIAI using only 50% of the original samples and sampling matrices (a)-(c).

from the limited bandwidth of the ADC and/or from an extended laser linewidth. In our setting, we relate the remaining uncertainty in the temporal width of the reflections to the effective receiver bandwidth,  $\Delta f$ . Hence, as an auxiliary global parameter, the value of  $\Delta f$  that correctly specifies the width of the reflections defines the correct dictionary parameter. Since  $\Delta f$  is unknown, we consider  $\hat{\theta} = \widehat{\Delta f}$  directly, rather than the ratio  $\widehat{\Delta f} / \Delta f$ . The total search range for  $\theta$  covers dictionaries with coherence distances  $9 \leq \hat{d}_c \leq 89$ . The correct value yields dictionaries with  $12 \leq d_c \leq 30$ . Besides, there are a few distortions that are not captured by the model in Section 5.1 such as the skew shape of the reflections. This may result from a different rise and fall time in the temporal response of the PD. Nonetheless,  $\mathbf{s}$ ,  $\theta$  and  $\mathbf{x}$  can still be estimated which indicates some robustness to model deviations. The rows in Fig. 8 show the performance of PDL-OIAI and PDL-OMP using the sampling matrices (a)-(c), respectively. The left column depicts the raw sensor signal,  $\mathbf{r}$ , after photodetection and A/D conversion. For the second reflection, the median of the estimated scaled atoms is shown (solid and dashed line). The shaded areas represent the 85% confidence intervals of the atom. The right column shows the median of the corresponding sparse coefficients along with the error bars corresponding to the 85% confidence intervals for  $\hat{\mathbf{x}}_{\mathcal{S}}$ . For the sparse signal, the shaded areas represent the 85% confidence intervals for  $\mathbf{s}$ . Since  $d_c$  is not too large and the SNR is relatively high, the *average* performance of both methods is not significantly different. Yet, the reflection delays,  $\hat{\mathbf{s}}$ , identified by PDL-OIAI are more accurate than those of PDL-OMP. Also,  $\hat{\mathbf{x}}_{\mathcal{S}}$  yielded by PDL-OIAI adheres closer

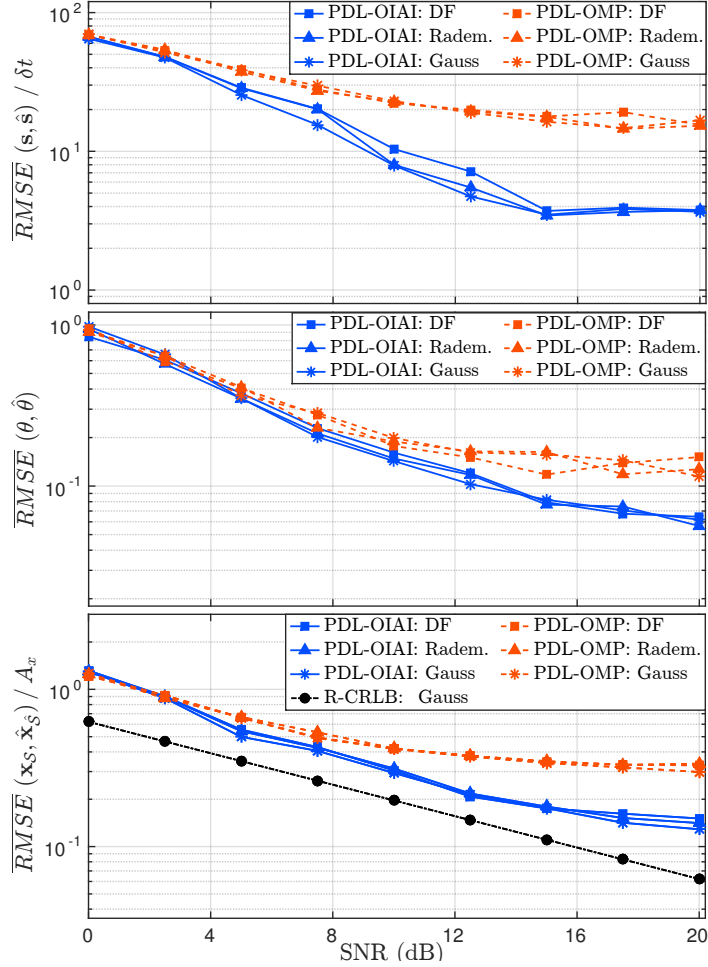


Figure 7: Performance of PDL-OMP and PDL-OIAI using only 20% of the original samples and sampling matrices (a)-(c).

to the amplitudes of the acquired signal. This is verified by much narrower confidence intervals of the support and amplitude estimates in the case of PDL-OIAI. Comparing the acquired data to the estimated atoms,  $\hat{\theta}$  obtained by PDL-OMP tends to be too small, which results in reflections that are broader than those of the sensor data. For the sampling matrices (a)-(c), the medians and 85% confidence regions,  $\Delta_{85\%}$ , of  $\hat{\theta}$  are shown in Table 2.

## 6 Discussion

By simulations and experimental data we show how the CS-DL framework can be truncated to match a particular sensor setup when a parametric model for the received signal is available. This enables the application of CS-DL to a wider range of applications akin to fiber-optic sensing such as laser ranging [11] or tomography [95], where reflection delays need to be estimated in a similar fashion. In order to apply CS-DL to a particular system, we assume a generic modular architecture and describe the core system in terms of an LTI model. Given that such a model is applicable and describes the system sufficiently accurately, other LTI components may be added, removed or exchanged. Hence, it can be customized to suit various system setups.

We use different sampling matrices to describe the CS acquisition process and to significantly reduce the number of acquired samples  $M \ll L$ , which is supported by simulations and experimental results.

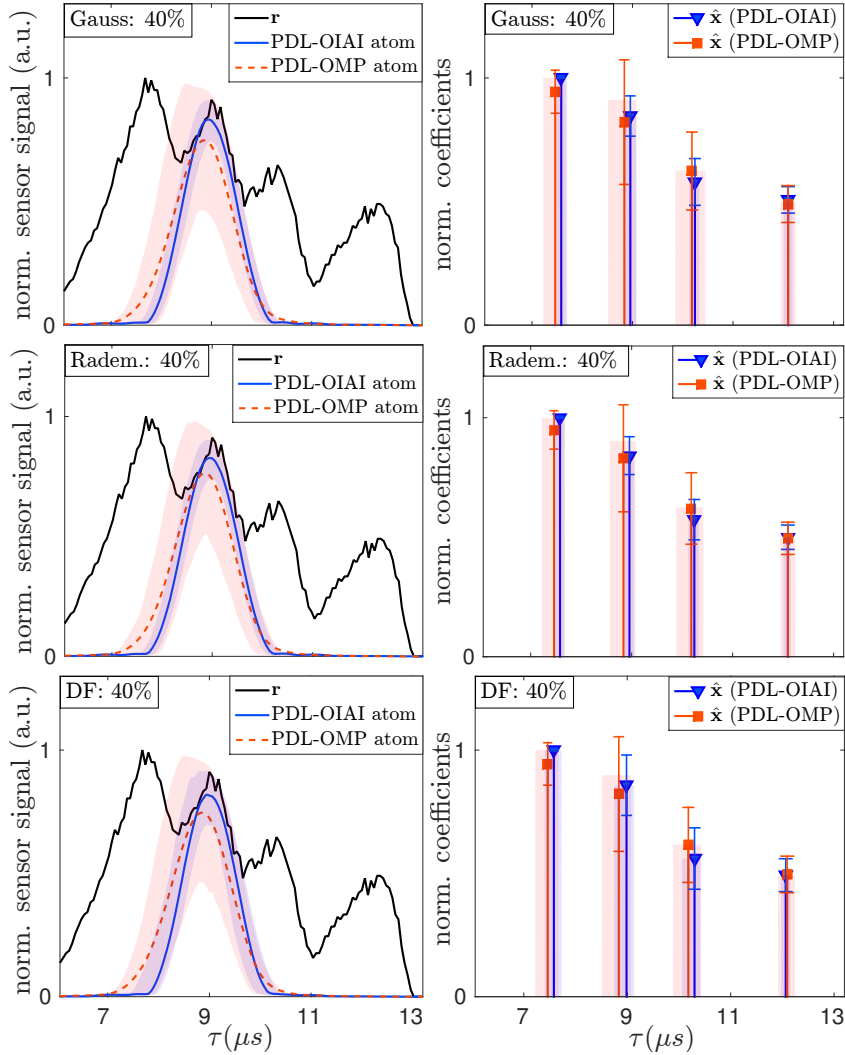


Figure 8: Real data example: Sensor signal with median of one estimated atom (left), median of the estimated support and amplitudes of  $\hat{\mathbf{x}}$  (right). For both algorithms, the shaded areas and the error bars correspond to the 85% confidence intervals.

Although sampling with Gaussian weights is most informative, all sampling matrices yield similar performance. We ascribe this observation to the high sparsity level imposed by the proposed dictionary structure. That is, only one atom per sub-dictionary can be active by definition. Binary matrices are especially favorable as they are easier to implement in hardware than a Gaussian matrix. For example, negative projections can be realized using a simple inverter. A full sampling matrix, e.g. a Rademacher matrix, describes a uniform sampling process (before compression). In order to lower the sampling rate, the receiver may be equipped with several parallel ADC branches. For example, uniform samples at rate  $f_s$  can be acquired by  $P$  parallel ADCs working at constant rate  $f_s/P$  [82]. Moreover, the *average* sampling rate can be further reduced by non-uniform sampling, which is described by a sparse sampling matrix. Besides the low storage requirements of sparse DF matrices [1], they have a high probability of zero projection (2/3 of all samples need not be acquired). This reduces the average sampling rate by  $\approx 66\%$ . In certain cases, non-uniform sampling can be further exploited to lower the hardware costs. That is, for uniform sampling,  $P$  parallel ADCs are required to reduce the sampling rate by factor  $P$ . However, if some positions of the full sampling grid are not occupied,  $\tilde{P} < P$  ADCs

Table 2: Medians and 85%-confidence ranges of the estimated receiver bandwidths  $\widehat{\Delta f}$  (in MHz) for the experimental data set using CS matrices (a)-(c) with  $M/L = 40\%$ .

Algorithm	Measure	Gaussian	Radem.	DF
<b>PDL-OMP</b>	Median	1.6560	1.6555	1.6458
	$\Delta_{85\%}$	0.2565	0.2397	0.3727
<b>PDL-OIAI</b>	Median	1.6545	1.6574	1.6371
	$\Delta_{85\%}$	0.8139	0.8115	0.7745

are sufficient. For example, if the sampling grid is sparse and every sequence of 4 samples in the rows of  $\Phi$  has either the pattern 0100 or 0010 (or a common cyclic shift), 2 parallel ADCs at rate  $f_s/4$  are sufficient as there are always at least 2 subsequent unoccupied positions.

It is evident from the previous results that PDL-OIAI is a viable tool for sparse estimation and PDL, yielding accurate estimates for  $\mathcal{S}$  and  $\theta$ . In addition, the sparse coefficients  $\hat{\mathbf{x}}_{\mathcal{S}}$  can be estimated with a performance close to the CRLB. Therefore, the results of PDL-OIAI are comparable to those of the  $\ell_p$ -RLS method in [7], which involves the solution of a non-convex optimization problem. By extending the parametric approaches in [56, 95], we show how PDL-OIAI performs AM-based PDL in the case of a composite dictionary structure with strong atom coherence and with additional uncertainty in the dictionary parameters. Different from the methods in [7, 54, 73], PDL-OIAI involves dictionary pre-conditioning, i.e. IAI mitigation, to handle severe dictionary coherence. Regarding the sparse estimation stage, this allows us to use a simple greedy algorithm rather than solving an additional optimization problem in each AM iteration. The necessity of such pre-conditioning in OMP-based sparse estimation with strong dictionary coherence becomes clear by comparing PDL-OIAI and PDL-OMP in the previous simulations. Thus, supporting the work in [94], we underline the benefits of IAI mitigation in the context of AM-based PDL. In particular, we show that it significantly reduces the coherence distance of the dictionary and, at the same time, maintains the correspondence between the locations of the sparse support and the physical quantities to be estimated (reflection delays). In addition, PDL-OIAI shows a certain robustness to model deviations as it obtains accurate estimates although the data exhibits some features that are not explicitly modeled (e.g. the skew shape of the reflections).

Using a parametric dictionary, the DL problem reduces to estimating a set of parameters rather than estimating the complete dictionary atoms as in [33, 3, 81]. Our model benefits from an analytic expression which is convenient to handle and allows to model complicated behavior only by tuning parameters. When the dictionary is created from a parametric model, prior knowledge of the dictionary structure such as shift-invariance can be exploited. Moreover, a parametric dictionary is storage-efficient since only the generating function and its parameters need to be stored. Nevertheless, a full sensing dictionary,  $\mathbf{W}$ , has to be determined and stored when  $d_c$  is too large. Yet, it remains the advantage that  $\hat{\mathbf{x}}$ , estimated from  $\mathbf{W}$ , can be used to estimate the desired quantities in terms of  $\mathbf{A}$  directly in the sparse domain. The atoms of a *non*-parametric dictionary, in turn, usually do not retain a physical interpretation. Our proposed dictionary is based on a general composite structure as in [31, 27, 19] but specifies one individual shift-invariant sub-dictionary for each FBG reflection. This particular structure promotes a high sparsity level since only one atom is active in each sub-dictionary. Moreover, it establishes an immediate relation between  $\mathcal{S}$  and the reflection delays.

Apart from the advantages of CS-DL and PDL-OIAI there are some drawbacks and limitations to be mentioned. One limitation is that, by subsequently minimizing the residual for individual parameters, only locally optimal estimates can be obtained for the dictionary parameters. Moreover, the contributions of different parameters might have similar impact on the residual so that not all parameters can be independently estimated. If the primary purpose is to obtain a correct sparse representation, one may define one auxiliary parameter as a function of similar or indistinguishable parameters that

describes their joint contribution to the property to be estimated. In our analysis, we defined the effective receiver bandwidth in order to estimate the width of the temporal reflections. A drawback of PDL-OIAI is its high computational complexity as compared to PDL-OMP. Yet, when  $d_c$  is too high, PDL-OMP does not yield accurate results which rationalizes the higher efforts for IAI mitigation. Also, simulations show that good performance is achieved when  $\mathbf{W}$  is calculated only once in the first OMP iteration, resulting in a significant speedup that can be further improved by computing the atoms of  $\mathbf{W}$  in parallel. Another drawback is the sensitivity of PDL-OIAI to the regularization parameter for IAI mitigation. It takes some initial efforts to determine a good value but this has to be done only once for a certain setting prior to the actual sensing process.

Finally, we would like to mention possible extensions that may improve the estimation performance. PDL-OIAI is generally capable of processing multiple observations in (5), i.e.  $\mathbf{y}(rT_{\text{sw}})$ ,  $r = 1, \dots, R_{T_{\text{sw}}}$ . Assuming that they all belong to the same stationary perturbation profile of the fiber, the sensitivity to noise can be reduced and some additional structure can be exploited, e.g. group-sparsity [46] across the sparse coefficients  $\mathbf{x}(rT_{\text{sw}})$ . Then, the model in (5) is rewritten as  $\mathbf{Y} = \mathbf{B}\mathbf{X} + \mathbf{N}$ , where  $\mathbf{Y}, \mathbf{X}, \mathbf{N}$  are matrices that consist of  $R_{T_{\text{sw}}}$  columns, each corresponding to one set of CS samples. A similar multi-snapshot technique has been proposed in [60], along with an appropriate formulation of the sparse estimation problem. Finally, due to the fact that OMP only selects one atom per iteration, it is not very sensitive to off-grid problems. Therefore, one may first use a coarser grid, i.e. smaller  $N$ , to yield a rough guess of the sparse support and then iteratively refine the grid to improve the precision to a certain level as in [60, 91]. This can reduce the dimensionality of the problem and the computational load.

## 7 Conclusion

We present a generic compressed sampling and dictionary learning framework, i.e. CS-DL, for WDM-based quasi-distributed fiber-optic sensing. CS-DL does not dictate a particular system setup but requires a generative parametric model for the observed signal. Imperfect prior knowledge can be incorporated in terms of uncertain global or local parameters. These parameters may have a direct physical significance or describe the joint impact of several (possibly indistinguishable) parameters on a certain quantity of interest. The viability of CS-DL is shown in a practical example, where the generic framework is truncated to suit a particular system setup. Herein, the effective receiver bandwidth represents a global parameter that determines the temporal width of the reflections. The basic model for this system can be further customized to cover a wider range of setups under the premise that they have a modular architecture and can be described by concatenated linear time-invariant components. Our model is employed to generate a parametric dictionary,  $\mathbf{A}$ , to be utilized by PDL-OIAI for sparse estimation and DL. The dictionary structure associates the sparse support with the reflection delays and allows for estimating the delays directly in the sparse domain. This structure promotes high sparsity levels (i.e. small  $K$ ) but also exhibits strong atom coherence which aggravates the sparse estimation performance. We introduce the coherence distance as an auxiliary measure to emphasize variations in  $\delta t$  and  $\theta$  when  $K$  is small. PDL-OIAI follows an AM approach to sparse estimation and DL. It is designed for parametric dictionaries and additionally incorporates IAI mitigation. Based on  $\mathbf{A}$ , IAI mitigation yields a modified sensing dictionary,  $\mathbf{W}$ , which has a significantly lower coherence distance but maintains the physical correspondence to the reflection delays. That is,  $\text{supp}\{\hat{\mathbf{x}}\}$  obtained from  $\mathbf{W}$  represents an estimate for the reflection delays in terms of  $\mathbf{A}$ . Using a sparse (binary) sampling matrix, the number of samples to be processed is substantially reduced and the average sampling rate is lowered without significant performance loss. Moreover, the performance of estimating the sparse coefficients in  $\mathbf{x}$  at the support locations is close to the CRLB. At the stage of DL, PDL-OIAI obtains locally optimal estimates for the uncertain dictionary parameters. The efficacy of PDL-OIAI is supported by an empirical performance analysis. Its applicability is further verified for experimental data, where we observe some robustness to distortions that are not captured by the model. Drawbacks of this method are an increased computational complexity due to IAI mitigation, the sensitivity to the regularization parameter, and the restriction to locally optimal dictionary parameter estimates. Also, not all parameters can be independently estimated. The problem of computational load can

be alleviated by parallel processing and by using a fixed sensing dictionary. Finally, a comparison to a reference method, PDL-OMP, sustains the necessity of IAI mitigation and rationalizes the higher computational efforts.

In a consecutive investigation, the amplitudes,  $\hat{\mathbf{x}}_S$ , can be incorporated in PDL-OIAI to improve the estimation performance, since they also carry information of the traveling delay. Further, efficient updating methods may be developed to directly process subsequent sets of CS samples.

## References

- [1] D. Achlioptas. Database-friendly random projections: Johnson-lindenstrauss with binary coins. *J. Comput. Syst. Sci.*, 66(4):671–687, 2003.
- [2] A. Agarwal, A. Anandkumar, P. Jain, P. Netrapalli, and R. Tandon. Learning sparsely used overcomplete dictionaries. *J. Mach. Learn. R. Workshop (JMLR)*, 35:1–15, 2014.
- [3] M. Aharon, M. Elad, and A. Bruckstein. K-SVD: An algorithm for designing overcomplete dictionaries for sparse representation. *IEEE Trans. Signal Process.*, 54(11):4311–4322, 2006.
- [4] S. B. Alexander. *Optical Communication Receiver Design*. SPIE, 1997.
- [5] S. Arora, R. Ge, and A. Moitra. New algorithms for learning incoherent and overcomplete dictionaries. *J. Machine Learn. R.: Workshop and Conf. Proc.*, 35:1–28, 2014.
- [6] M. Ataee, H. Zayyani, M. Babaie-Zadeh, and C. Jutten. Parametric dictionary learning using steepest descent. In *IEEE Int. Conf. Acoust., Speech, Signal Process. (ICASSP)*, pages 1978–1981, Mar 2010.
- [7] C. D. Austin, J. N. Ash, and R. L. Moses. Dynamic dictionary algorithms for model order and parameter estimation. *IEEE Transactions on Signal Processing*, 61(20):5117–5130, Oct 2013.
- [8] C. D. Austin, E. Ertin, J. N. Ash, and R. L. Moses. On the relation between sparse sampling and parametric estimation. In *IEEE 13th Digit. Signal Process. Workshop and 5th IEEE Signal Process. Edu. Workshop (DSP/SPE)*, pages 387–392, Jan 2009.
- [9] C. D. Austin, R. L. Moses, J. N. Ash, and E. Ertin. On the relation between sparse reconstruction and parameter estimation with model order selection. *IEEE J. Sel. Top. Signal Process.*, 4(3):560–570, Jun 2010.
- [10] A. Abd El Aziz, W.P. Ng, Z. Ghassemlooy, M.H. Aly, and R. Ngah. Soa gain uniformity improvement employing a non-uniform biasing technique for ultra-high speed optical routers. In *7th Int. Symp. Commun. Syst. Netw. and Digit. Signal Process. (CSNDSP)*, pages 642–647, Jul 2010.
- [11] W. R. Babbitt, Z. W. Barber, and C. Renner. Compressive laser ranging. *Opt. Lett.*, 36(24):4794–4796, Dec 2011.
- [12] R.G. Baraniuk. Compressive sensing [lecture notes]. *IEEE Signal Process. Mag.*, 24(4):118–121, Jul 2007.
- [13] A. Beck and L. Tetruashvili. On the convergence of block coordinate descent type methods. *SIAM J. Optim.*, 23(4):2037–2060, 2013.
- [14] Z. Ben-Haim and Y. C. Eldar. The Cramer-Rao bound for estimating a sparse parameter vector. *IEEE Trans. Signal Process.*, 58(6):3384–3389, Jun 2010.
- [15] T. Blumensath and M. Davies. Sparse and shift-invariant representations of music. *IEEE Trans. on Audio, Speech, Language Process.*, 14(1):50–57, Jan 2006.
- [16] M. Born and E. Wolf. *Principles of Optics*. Cambridge University Press, 7 edition, 1999.

- [17] T.T. Cai and L. Wang. Orthogonal matching pursuit for sparse signal recovery with noise. *IEEE Trans. Inf. Theory*, 57(7):4680–4688, Jul 2011.
- [18] E.J. Candes. The restricted isometry property and its implications for compressed sensing. *C.R. Math.*, 346:589–592, 2008.
- [19] E.J. Candes, Y.C. Eldar, D. Needell, and P. Randall. Compressed sensing with coherent and redundant dictionaries. *Appl. Comput. Harmon. Anal.*, 31:59–73, Jul 2011.
- [20] E.J. Candes and T. Tao. Decoding by linear programming. *IEEE Trans. Inf. Theory*, 51(12):4203–4215, Dec 2005.
- [21] E.J. Candes and M.B. Wakin. An introduction to compressive sampling. *IEEE Signal Process. Mag.*, 25(2):21–30, Mar 2008.
- [22] Z. Chen and Y. Wu. Robust dictionary learning by error source decomposition. In *IEEE Int. Conf. Comput. Vision*, pages 2216–2223, Dec 2013.
- [23] B. Culshaw. Optical fiber sensor technologies: Opportunities and - perhaps - pitfalls. *J. Lightwave Technol.*, 22(1):39, Jan 2004.
- [24] B. Culshaw and A. Kersey. Fiber-optic sensing: A historical perspective. *J. Lightwave Technol.*, 26(9):1064–1078, May 2008.
- [25] B. Culshaw, G. Thursby, D. Betz, and B. Sorazu. The detection of ultrasound using fiber-optic sensors. *IEEE Sensors J.*, 8(7):1360–1367, Jul 2008.
- [26] M. A. Davenport and M. B. Wakin. Analysis of orthogonal matching pursuit using the restricted isometry property. *IEEE Trans. Inf. Theory*, 56(9):4395–4401, Sep 2010.
- [27] D.L. Donoho and M. Elad. Optimally sparse representation in general (nonorthogonal) dictionaries via  $\ell_1$ -minimization. *Proc. Nat. Acad. Sci. (PNAS)*, 100(5):2197–2202, 2003.
- [28] D.L. Donoho and X. Huo. Uncertainty principles and ideal atomic decomposition. *IEEE Trans. Inf. Theory*, 47(7):2845–2862, Nov 2001.
- [29] M. Elad. Optimized projections for compressed sensing. *IEEE Trans. Signal Process.*, 55(12):5695–5702, Dec 2007.
- [30] M. Elad. *Sparse and Redundant Representations: From Theory to Applications in Signal and Image Processing*. Springer, 2010.
- [31] M. Elad and A.M. Bruckstein. A generalized uncertainty principle and sparse representation in pairs of bases. *IEEE Trans. Inf. Theory*, 48(9):2558–2567, Sep 2002.
- [32] Y.C. Eldar and G. Kutyniok, editors. *Compressed Sensing: Theory and Applications*. Cambridge University Press, 2012.
- [33] K.I. Engan, K. Skretting, and J.H. Husoy. Family of iterative LS-based dictionary learning algorithms, ILS-DLA, for sparse signal representation. *Digit. Signal Process.*, 17(1):32–49, 2007.
- [34] T. Erdogan. Fiber grating spectra. *J. Lightwave Technol.*, 15(8):1277–1294, Aug 1997.
- [35] S. Foucart and H. Rauhut. *A Mathematical Introduction to Compressive Sensing*. Birkhäuser, 2013.
- [36] K. Fyhn, M. F. Duarte, and S. H. Jensen. Compressive parameter estimation for sparse translation-invariant signals using polar interpolation. *IEEE Trans. Signal Process.*, 63(4):870–881, Feb 2015.

- [37] Y.R. Garcia, J.M. Corres, and J. Goicoechea. Vibration detection using optical fiber sensors. *J. Sensors*, page 12 pp, 2010.
- [38] M.E. Gehm and D.J. Brady. Compressive sensing in the EO/IR. *Appl. Opt.*, 54(8):C14–C22, Mar 2015.
- [39] A. Gilbert, S. Muthukrishnan, and M.J. Strauss. Approximation of functions over redundant dictionaries using coherence. In *Proc. 14th Annu. ACM-SIAM Symp. Discrete algorithms (SODA)*, pages 243–252, 2003.
- [40] N. A. Goodman and L. C. Potter. Pitfalls and possibilities of radar compressive sensing. *Appl. Opt.*, 54(8):C1–C13, Mar 2015.
- [41] R. Gribonval, R. Jenatton, and F. Bach. Sparse and spurious: Dictionary learning with noise and outliers. *IEEE Trans. Inf. Theory*, 61(11):6298–6319, Nov 2015.
- [42] R. Gribonval and M. Nielsen. Sparse representations in unions of bases. *IEEE Trans. Inf. Theory*, 49(12):3320–3325, Dec 2003.
- [43] T.L. Hansen, M.A. Badiu, B.H. Fleury, and B.D. Rao. A sparse Bayesian learning algorithm with dictionary parameter estimation. In *IEEE 8th Sensor Array and Multichannel Signal Process. Workshop (SAM)*, pages 385–388, June 2014.
- [44] M. A. Herman and T. Strohmer. High-resolution radar via compressed sensing. *IEEE Trans. Signal Process.*, 57(6):2275–2284, June 2009.
- [45] K. Hotate and K. Kajiwara. Proposal and experimental verification of bragg wavelength distribution measurement within a long-length fbg by synthesis of optical coherence function. *Opt. Express*, 16(11):7881–7887, May 2008.
- [46] J. Huang and T. Zhang. The benefit of group sparsity. *Ann. Statist.*, 38(4):1978–2004, Aug 2010.
- [47] E. Ip, A.P.T. Lau, D.J.F. Barros, and J.M. Kahn. Coherent detection in optical fiber systems. *Opt. Express*, 16(2):753–791, Jan 2008.
- [48] P. Jost, P. Vandergheynst, S. Lesage, and R. Gribonval. Learning redundant dictionaries with translation invariance property: the MoTIF algorithm. In B. Torresani R. Gribonval, L. Daudet, editor, *Workshop Signal Process. Adapt. Sparse Struct. Represent. (SPARS)*, pages 1–3, Rennes, France, 2005. Inria.
- [49] P. Jost, P. Vandergheynst, S. Lesage, and R. Gribonval. MoTIF: An efficient algorithm for learning translation invariant dictionaries. In *IEEE Int. Conf. on Acoust. Speech, Signal Process.*, volume 5, pages V–V, May 2006.
- [50] R. Kashyap. *Fiber Bragg Gratings*. AP, 2 edition, 2009.
- [51] A. D. Kersey. Optical fiber sensors for permanent downwell monitoring applications in the oil and gas industry. *IEICE Trans. Electron.*, E83-C:400–404, Mar 2000.
- [52] A.D. Kersey, M.A. Davis, H.J. Patrick, M. LeBlanc, K.P. Koo, C.G. Askins, M.A. Putnam, and E.J. Friebele. Fiber grating sensors. *J. Lightwave Technol.*, 15(8):1442–1463, Aug 1997.
- [53] H. Kogelnik. Theory of optical waveguides. In T. Tamir, editor, *Guided-Wave Optoelectronics*, volume 26 of *Springer Series in Electronics and Photonics*, pages 7–88. Springer, 1988.
- [54] M. Leigsnering, F. Ahmad, M. G. Amin, and A. M. Zoubir. Parametric dictionary learning for sparsity-based TWRI in multipath environments. *IEEE Trans. Aerosp. Electron. Syst.*, 52(2):532–547, Apr 2016.

- [55] M.S. Lewicki and T.J. Sejnowski. Learning overcomplete representations. *Neural Comput.*, 12(2):337–365, Feb 2000.
- [56] Y. Liang, M. Chen, H. Chen, C. Lei, P. Li, and S. Xie. Photonic-assisted multi-channel compressive sampling based on effective time delay pattern. *Opt. Express*, 21(22):25700–25707, Nov 2013.
- [57] Y.-P. Lin and P. P. Vaidyanathan. Periodically nonuniform sampling of bandpass signals. *IEEE Trans. Circuits Syst. II: Analog Digit. Signal Process.*, 45(3):340–351, Mar 1998.
- [58] C. Lu, J. Shi, and J. Jia. Online robust dictionary learning. In *IEEE Conf. Comput. Vision Pattern Recognit. (CVPR)*, pages 415–422, June 2013.
- [59] M. Lustig, D.L. Donoho, J.M. Santos, and J.M. Pauly. Compressed sensing MRI. *IEEE Signal Process. Mag.*, 25(2):72–82, Mar 2008.
- [60] D. Malioutov, M. Cetin, and A.S. Willsky. A sparse signal reconstruction perspective for source localization with sensor arrays. *IEEE Trans. Signal Process.*, 53(8):3010–3022, 2005.
- [61] Raymond M. Measures. *Structural Monitoring with Fiber Optic Technology*. AP, 2001.
- [62] R.M. Measures, M. LeBlanc, K. Liu, S. Ferguson, T. Valis, D. Hogg, R. Turner, and K. McEwen. Fiber optic sensors for smart structures. *Opt. Lasers Eng.*, 16:127–152, 1992. Special Issue on Optical Sensors for Aerospace Applications.
- [63] A. Mendez and T. Morse. *Specialty Optical Fibers Handbook*. Elsevier, 2007.
- [64] M. Mishali and Y.C. Eldar. Blind multiband signal reconstruction: Compressed sensing for analog signals. *IEEE Trans. Signal Process.*, 57(3):993–1009, Mar 2009.
- [65] M. Mishali, Y.C. Eldar, O. Dounaevsky, and E. Shoshan. Xampling: Analog to digital at subnyquist rates. *IET Circuits Devices Syst.*, 5(1):8–20, Jan 2011.
- [66] M. Mishali, Y.C. Eldar, and A.J. Elron. Xampling: Signal acquisition and processing in union of subspaces. *IEEE Trans. Signal Process.*, 59(10):4719–4734, Oct 2011.
- [67] W.W. Morey, G. Meltz, and W.H. Glenn. Fiber optic Bragg grating sensors. *Proc. SPIE 1169, Fiber Optic Laser Sensors VII*, 1169:p. 98, 1990.
- [68] H. Murayama, D. Wada, and H. Igawa. Structural health monitoring by using fiber-optic distributed strain sensors with high spatial resolution. *J. Photonic Sensors*, 3(4):355–376, 2013.
- [69] Y. Nakazaki and S. Yamashita. Fast and wide tuning range wavelength-swept fiber laser based on dispersion tuning and its application to dynamic FBG sensing. *Opt. Express*, 17(10):8310–8318, May 2009.
- [70] A. Othonos and K. Kalli. *Fiber Bragg Gratings: Fundamentals and Applications in Telecommunications and Sensing*. Artech House, 1999.
- [71] B. P. Pal. *Fundamentals Of Fibre Optics In Telecommunication And Sensor Systems*. New Age International, 2005.
- [72] V.M. Patel, G.R. Easley, D.M. Healy Jr., and R. Chellappa. Compressed synthetic aperture radar. *IEEE J. Sel. Topics Signal Process.*, 4(2):244–254, Apr 2010.
- [73] H. Raja, W. U. Bajwa, F. Ahmad, and M. G. Amin. Parametric dictionary learning for TWRI using distributed particle swarm optimization. In *Proc. IEEE Radar Conf.*, May 2016.
- [74] H. Rauhut, K. Schnass, and P. Vandergheynst. Compressed sensing and redundant dictionaries. *IEEE Trans. Inf. Theory*, 54(5):2210–2219, May 2008.

- [75] A. Rosenthal and M. Horowitz. Inverse scattering algorithm for reconstructing lossy fiber Bragg gratings. *J. Opt. Soc. Am. A*, 21(4):552–560, Apr 2004.
- [76] R. Rubinstein, A.M. Bruckstein, and M. Elad. Dictionaries for sparse representation modeling. *Proc. IEEE*, 98(6):1045–1057, Jun 2010.
- [77] S.J. Savory. Digital filters for coherent optical receivers. *Opt. Express*, 16(2):804–817, Jan 2008.
- [78] K. Schnass and P. Vandergheynst. Dictionary preconditioning for greedy algorithms. *IEEE Trans. Signal Process.*, 56(5):1994–2002, May 2008.
- [79] M. Seimetz. *High-Order Modulation for Optical Fiber Transmission: Phase and Quadrature Amplitude Modulation*. Springer, 2009.
- [80] J. Sheng, C. Yang, and M.C. Herbordt. Hardware-efficient compressed sensing encoder designs for WBSNs. In *IEEE High Perform. Extreme Comput. Conf. (HPEC)*, pages 1–7, Sep 2015.
- [81] K. Skretting and K. Engan. Recursive least squares dictionary learning algorithm. *IEEE Trans. Signal Process.*, 58(4):2121–2130, Apr 2010.
- [82] T. Strohmer and J. Tanner. Fast reconstruction algorithms for periodic nonuniform sampling with applications to time-interleaved ADCs. In *IEEE Int. Conf. Acoust. Speech Signal Process. (ICASSP)*, volume 3, pages III–881–III–884, Apr 2007.
- [83] K. Tamura and M. Nakazawa. Dispersion-tuned harmonically mode-locked fiber ring laser for self-synchronization to an external clock. *Opt. Lett.*, 21(24):1984–1986, Dec 1996.
- [84] J.A. Tropp. Greed is good: algorithmic results for sparse approximation. *IEEE Trans. Inf. Theory*, 50(10):2231–2242, Oct 2004.
- [85] E. Udd. Fiber optic smart structures. *Proc. IEEE*, 84(1):60–67, Jan 1996.
- [86] H. Venghaus, editor. *Wavelength Filters in Fibre Optics*, volume 123 of *Springer Series Opt. Sci.* Springer, 2006.
- [87] C. Weiss and A. M. Zoubir. Fiber sensing using ufwt-lasers and sparse acquisition. In *Proc. 21st Eur. Signal Process. Conf. (EUSIPCO)*, pages 1–5. EURASIP, 2013.
- [88] C. Weiss and A.M. Zoubir. Fiber sensing using wavelength-swept lasers: A compressed sampling approach. In *3rd Int. Workshop Compressed Sens. Theory Appl. Radar Sonar Remote Sens. (CoSeRa)*, pages 21–25, Jun 2015.
- [89] A.E. Willner and W. Shieh. Optimal spectral and power parameters for all-optical wavelength shifting: single stage, fanout, and cascability. *J. Lightwave Technol.*, 13(5):771–781, May 1995.
- [90] X. Xiong, C. Han, Q. Ding, L. Liu, and D. Li. A parallel delta-sigma ADC based on compressive sensing. In *IEEE Int. Conf. Electron. Devices Solid-State Circuits (EDSSC)*, pages 1–2, Jun 2013.
- [91] D. Xu, L. Du, and H. Liu. Radar signal parameter estimation with sparse Bayesian representation based on zoom-dictionary. In *IEEE Int. Conf. Comput Inf. Technol. (CIT)*, pages 123–128, Sep 2014.
- [92] M. Yaghoobi, L. Daudet, and M.E. Davies. Parametric dictionary design for sparse coding. In R. Gribonval, editor, *Signal Process. Adapt. Sparse Struct. Represent. (SPARS)*, Saint Malo, France, Apr 2009. Inria Rennes - Bretagne Atlantique.
- [93] S. Yamashita, Y. Nakazaki, R. Konishi, and O. Kusakari. Wide and fast wavelength-swept fiber laser based on dispersion tuning for dynamic sensing. *J. Sensors*, 2009:12, 2009.

- [94] R. Yang, Q. Wan, Y. Liu, and W. Yang. Adaptive inter-atom interference mitigation approach to sparse multi-path channel estimation. In *IEEE 71st Veh. Technol. Conf.*, pages 1–5, May 2010.
- [95] R. Yao, Q. Pian, and X. Intes. Molecular fluorescence tomography with structured light and compressive sensing. In *Opt. Life Sci.*, page JT3A.25. OSA, 2015.
- [96] A. Yariv. Coupled-mode theory for guided-wave optics. *IEEE J. of Quantum Electron.*, 9(9):919–933, Sep 1973.
- [97] S. Yin, P.B. Ruffin, and F.T.S. Yu, editors. *Fiber Optic Sensors*. CRC Press, 2 edition, 2008.
- [98] H. Yu and G. Wang. Compressed sensing based interior tomography. *Phys. Med. Biol.*, 54(9):2791, 2009.
- [99] Z. Yu, S. Hoyos, and B.M. Sadler. Mixed-signal parallel compressed sensing and reception for cognitive radio. In *IEEE Int. Conf. Acoust. Speech Signal Process. (ICASSP)*, pages 3861–3864, Mar 2008.
- [100] T. Zhang. Sparse recovery with orthogonal matching pursuit under RIP. *IEEE Trans. Inf. Theory*, 57(9):6215–6221, Sep 2011.

## 8 Acknowledgments

This work was supported by the 'Excellence Initiative' of the German Federal and State Governments and the Graduate School of Computational Engineering at Technische Universität Darmstadt. The authors thank Professor Shinji Yamashita and his group at The University of Tokyo, Japan, for kindly providing experimental data of the fiber sensor in [93].

## A CRLB for orthonormal matrices

In order to determine a lower bound for the CRLB with respect to the sensing matrix,  $\mathbf{B}$ , consider a positive semi-definite matrix  $\mathbf{H} = \mathbf{B}_S^T \mathbf{B}_S$  with eigenvalues  $\lambda_k \geq 0$ ,  $k = 1, \dots, K$ . Using Hadamard's inequality we find

$$\det(\mathbf{H}) = \prod_{k=1}^K \lambda_k \leq \prod_{k=1}^K h_{kk} = \prod_{k=1}^K \tilde{\lambda}_k = \det(\mathbf{D}), \quad (36)$$

where  $h_{kk}$  are the diagonal entries of  $\mathbf{H}$  and  $\tilde{\lambda}_k$  are the eigenvalues of some diagonal matrix  $\mathbf{D}$ . Further, for  $\mathbf{H}^{-1}$  we find

$$\det(\mathbf{H}^{-1}) = \prod_{k=1}^K \frac{1}{\lambda_k} \geq \prod_{k=1}^K \frac{1}{\tilde{\lambda}_k} = \det(\mathbf{D}^{-1}) \quad (37)$$

Therefore, the lowest CRLB is achieved when  $\mathbf{H}$  is a diagonal, i.e. when the columns of  $\mathbf{B}$  are orthogonal. Then,  $\mathbf{H} = \mathbf{D}$  and equality holds in (36) and (37). Since the columns in  $\mathbf{B}$  are normalized, i.e.  $\|\mathbf{b}_k\|_2^2 = \tilde{\lambda}_k = 1$ , we obtain the expression

$$E\{\|\hat{\mathbf{x}}_{ub} - \mathbf{x}\|_2^2\} \geq \sigma_n^2 \sum_{k=1}^K \frac{1}{\tilde{\lambda}_k} = K \sigma_n^2. \quad (38)$$